Caenorhabditis elegans processes sensory information to choose between freeloading and self-defense strategies

Jodie Schiffer[1], Francesco Servello[1], William Heath[1], Francis Raj Gandhi Amrit[2], Stephanie Stumbur[1], Sean Johnsen[1], Julian Stanley[1], Hannah Tam[1], Sarah Brennan[1], Natalie McGowan[1], Abigail Vogelaar[1], Yuyan Xu[1], William Serkin[1], Arjumand Ghazi[2,3], and Javier Apfeld[1*]

[1] Biology Department, Northeastern University, Boston, Massachusetts, United States of America.

[2] Department of Pediatrics, University of Pittsburgh School of Medicine, Pittsburgh, Pennsylvania, United States of America.

[3] Departments of Developmental Biology and Cell Biology and Physiology, University of Pittsburgh School of Medicine, Pittsburgh, Pennsylvania, United States of America.

* For correspondence: j.apfeld@northeastern.edu

Abstract

Hydrogen peroxide is the preeminent chemical weapon that organisms use for combat. Individual cells rely on conserved defenses to prevent and repair peroxide-induced damage, but whether similar defenses might be coordinated across cells in animals remains poorly understood. Here, we identify a neuronal circuit in the nematode *Caenorhabditis elegans* that processes information perceived by two sensory neurons to control the induction of hydrogen-peroxide defenses in the organism. We found that catalases produced by *Escherichia coli*, the nematode's food source, can deplete hydrogen peroxide from the local environment and thereby protect the nematodes. In the presence of *E. coli*, the nematode's neurons signal via TGFβ-insulin/IGF1 relay to target tissues to repress expression of catalases and other hydrogen-peroxide defenses. This adaptive strategy is the first example of a multicellular organism modulating its defenses when it expects to freeload from the protection provided by molecularly orthologous defenses from another species.

Introduction

Bacteria, fungi, plants, and animal cells have long been known to excrete large quantities of hydrogen peroxide to attack their prey and pathogens (Avery and Morgan, 1924). Hydrogen peroxide is also a dangerous byproduct of aerobic respiration (Chance et al., 1979). Cells rely on highly conserved defense mechanisms to degrade hydrogen peroxide and avoid the damage that hydrogen peroxide inflicts on their proteins, nucleic acids, and lipids (Mishra and Imlay, 2012). The extent to which these protective defenses are coordinated across cells in animals is poorly understood.

In the present study, we used the nematode *C. elegans* as a model system to explore whether hydrogen-peroxide protective defenses are coordinated across cells. We focused on the role of sensory neurons in this coordination because sensory circuits in the brain collect and integrate information from the environment, enabling animals to respond to environmental change. Specific sensory neurons enable nematodes to smell, taste, touch, and sense temperature and oxygen levels (Bargmann and Horvitz, 1991a; Chalfie et al., 1985; Gray et al., 2004; Mori and Ohshima, 1995; White et al., 1986). This information is integrated rapidly by interneurons to direct the nematode's movement towards favorable environmental cues and away from harmful ones (Kaplan et al., 2018). Nematodes also use sensory information to modify their development, metabolism, lifespan, and heat defenses (Apfeld and Kenyon, 1999; Bargmann and Horvitz, 1991b; Mak et al., 2006; Prahlad et al., 2008). Understanding how sensory circuits in the brain regulate hydrogen-peroxide defenses in *C. elegans* may provide a template for understanding how complex animals coordinate their cellular defenses in response to the perceived threat of hydrogen-peroxide attack.

Using a systematic neuron-specific genetic-ablation approach, we identified ten classes of sensory neurons that regulate sensitivity to harmful peroxides in *C. elegans*. We found that the two ASI sensory neurons of the amphid, the major sensory organ of the nematode, initiate a multistep hormonal relay that decreases the nematode's hydrogen peroxide defenses: a DAF-7/TGFβ signal from ASI is received by multiple sets of interneurons, which independently process this information and then relay it to target tissues via insulin/IGF1 signals. Interestingly, this neuronal circuit lowers the action of endogenous catalases and other hydrogen-peroxide defenses within the worm in response to perception and ingestion of *E. coli*, the nematode's primary food source in laboratory experiments. We show that *E. coli* express orthologous defenses that degrade hydrogen peroxide in the environment and that *C. elegans* does not need to induce catalases and other hydrogen-peroxide defenses when *E. coli* is abundant.

Thus, this neuronal circuit enables the nematodes to lower their own defenses upon sensing bacteria that can provide protection. In the microbial battlefield, nematodes use a sensory-neuronal circuit to determine whether to defend themselves from hydrogen peroxide attack or to freeload off protective defenses from another species.

Results

Sensory neurons regulate peroxide resistance in *C. elegans*

C. elegans is highly sensitive to the lethal effects of peroxides. Under standard laboratory conditions, wild-type nematodes have an average lifespan of approximately 15 days (Kenyon et al., 1993). In contrast, when grown in the presence of peroxides (6 mM tert-butyl hydroperoxide, tBuOOH), the average lifespan of these nematodes is reduced to less than 1 day (Fig. 1A) (An et al., 2005). Previously, we determined the peroxide resistance of nematodes by measuring their lifespan with high temporal resolution in the presence of 6 mM tBuOOH (Stroustrup et al., 2013).

To investigate whether sensory neurons might regulate the nematode's peroxide defenses, we measured peroxide resistance in mutant animals with global defects in sensory perception. We first examined *osm-5* cilium structure mutants, which lack neuronal sensory perception due to defects in the sensory endings (cilia) of most sensory neurons (Perkins et al., 1986). These mutants exhibited a 45% increase in peroxide resistance relative to wild-type controls (Fig. 1A and Table S1). Next, we examined *tax-2* and *tax-4* cyclic GMP-gated channel mutants, which are defective in the transduction of several sensory processes including smell, taste, oxygen, and temperature sensation (Coburn and Bargmann, 1996; Komatsu et al., 1996). These two

mutants also exhibited large increases in peroxide resistance compared to wild-type controls (Figs. 1A and S1A, and Table S1). Together, these observations indicate that neuronal sensory perception plays a role in regulating peroxide resistance in nematodes.

In *C. elegans* hermaphrodites, 60 ciliated and 12 non-ciliated neurons perform most sensory functions (White et al., 1986). To identify which of these sensory neurons influence the nematode's peroxide resistance, we systematically measured peroxide resistance in a collection of strains in which specific sensory neurons have been genetically ablated via neuron-specific expression of caspases (Chelur and Chalfie, 2007) or, in one case, via mutation of a neuron-specific fate determinant (Chang et al., 2003; Uchida et al., 2003). Overall, our neuron-ablation collection covered 44 ciliated and 10 non-ciliated neurons, including each of the 12 pairs of ciliated neurons that make up the two amphids (the major sensory organs), 8 of the 13 classes of non-amphid ciliated neurons, and 6 of the 7 classes of non-ciliated sensory neurons (Table S9). Individual ablation of ASI, ASG, ASK, AFD, AWC, IL2 and joint ablation of ADE, PDE, and CEP increased the nematode's peroxide resistance by up to 61% (Figs. 1A-B and S1B-C, and Table S1), whereas individual ablation of ASJ and AWA, and joint ablation of URX, AQR, and PQR reduced peroxide resistance by up to 16% (Fig. 1A-B). The remainder of the neurons tested—ADF, ADL, ASE, ASH, AWB, OLL, and joint ablation of ALM, PLM, AVM, PVM, FLP, and PVD—did not affect peroxide resistance (Figs. 1A, 1C and S1D-G, and Table S1). Altogether, we found that ten classes of sensory neurons can positively or negatively modulate peroxide resistance (Fig. 1B). These neurons are known to respond to diverse stimuli, including smell, taste, touch, temperature, and oxygen levels (Fig. 1C), suggesting that nematodes might adjust their peroxide resistance in response to multiple types of sensory information.

ASI sensory neurons regulate peroxide resistance via DAF-7/TGFβ signaling

Among all neuronal ablations tested, ablation of ASI, a pair of neurons that sense taste and temperature, caused the largest increase in peroxide resistance (Fig. 1A). Thus, we focused on the role of the ASI neuronal pair. ASI neurons secrete many peptide hormones, including DAF-7 (Meisel et al., 2014; Ren et al., 1996), a transforming growth factor β (TGFβ) hormone that regulates feeding, development, metabolism, and lifespan (Dalfo et al., 2012; Greer et al., 2008; Ren et al., 1996; Shaw et al., 2007). To determine whether DAF-7/TGFβ signaling also regulates peroxide resistance, we examined mutants in *daf-7*. We found that *daf-7(ok3125)* null and *daf-7(e1372)* loss-of-function mutations increased peroxide resistance two-fold relative to wild-type controls (Figs. 2A, 2B, and S2A-D, and Table S2). Reintroducing the *daf-7(+)* gene into *daf-7(ok3125)* mutants restored peroxide resistance to wild-type levels (Fig. 2B and Table S2). Moreover, expression of *daf-7(+)* only in the ASI neurons was sufficient to reduce the peroxide resistance of *daf-7(ok3125)* mutants to wild-type levels (Fig. 2C and Table S2). *daf-7* is also expressed at a low level in ASJ, another pair of chemosensory neurons (Meisel et al., 2014), and expression of *daf-7(+)* only in ASJ rescued the increased peroxide resistance of *daf-7(ok3125)* mutants (Fig. 2D and Table S2). Thus, expression of *daf-7* in ASI or ASJ was sufficient to confer normal peroxide resistance. Because ablation of ASI increased peroxide resistance but ablation of ASJ did not (Fig. 1A), we reason that ASI neurons are the source of DAF-7 that regulates the nematode's peroxide resistance.

We next asked whether DAF-7/TGFβ from ASI might regulate resistance to additional toxic chemicals from the environment that are not peroxides or directly generate peroxides. We tested sensitivity of *daf-7* mutants to arsenite (a toxic metalloid), paraquat (a redox-cycling herbicide), and dithiothreitol/DTT (a reducing agent). Compared with wild-type animals, *daf-7(ok3125)* mutants had similar survival in 5 mM arsenite, 25 mM dithiothreitol, and 75 mM paraquat (Figs. 2A and 2E-G, and Table S2). Therefore, the DAF-7/TGFβ signal from ASI is a specific regulator of peroxide resistance in the worm.

147

148 **Interneurons must reach a consensus to increase peroxide resistance in response to**
149 **DAF-7/TGFβ from ASI**

150

151 DAF-7/TGFβ signals via the Type 1 TGFβ receptor DAF-1 (Georgi et al., 1990) to regulate
152 multiple downstream processes (Dalfo et al., 2012; Greer et al., 2008; Ren et al., 1996; Shaw et
153 al., 2007). Signaling through the DAF-1 receptor inactivates the transcriptional activity of a
154 complex between the receptor-associated coSMAD, DAF-3, and the Sno/Ski factor, DAF-5 (da
155 Graca et al., 2004; Patterson et al., 1997; Tewari et al., 2004). We found that a similar signal-
156 transduction pathway regulates peroxide resistance. *daf-1(m40)* loss-of-function mutants
157 showed a two-fold increase in peroxide resistance (Fig. 3A and Table S3), and the increase in
158 peroxide resistance of *daf-7* and *daf-1* mutants was almost completely abrogated by null or loss-
159 of-function mutations in either *daf-3* or *daf-5* (Figs. 3A and S3A-C, and Table S3). The *daf-*
160 *3(mgDf90)* null mutation also suppressed the increase in peroxide resistance of ASI-ablated
161 worms (Fig. 3B and Table S3). Therefore, the ASI neurons normally function to lower peroxide
162 resistance in the worm using a canonical TFGβ signaling pathway.

163

164 To determine which cells receive the DAF-7/TFGβ signal from the ASI neurons to regulate
165 peroxide resistance, we restored *daf-1(+)* gene expression in specific subsets of neurons using
166 cell-type specific promoters in *daf-1(m40)* mutants (Fig. 3C). DAF-1/TFGβ receptor is expressed
167 broadly in the nervous system and in the distal-tip cells of the gonad (Gunther et al., 2000). Pan-
168 neuronal expression of *daf-1(+)* with the *egl-3* promoter lowered peroxide resistance in *daf-1*
169 mutants to the same extent as did expressing *daf-1(+)* with the endogenous *daf-1* promoter
170 (Figs. 3D and 3E, and Table S3). Reconstituting *daf-1(+)* expression in all ciliated neurons
171 (except BAG and FLP) using the *osm-6* promoter had a minimal effect on peroxide resistance
172 (Fig. 3F and Table S3), indicating that *daf-1* functions in non-ciliated neurons. Expression of *daf-*

1(+) in multiple sets of non-ciliated interneurons and pharyngeal neurons using the *flp-1*, *tdc-1*, *glr-1*, or *glr-8* promoters lowered peroxide resistance to a similar extent as pan-neuronal expression of *daf-1(+)* in *daf-1* mutants (Figs. 3G-I and S3D, and Table S3), while directed *daf-1(+)* expression in nine pharyngeal neurons using the *glr-7* promoter did not affect peroxide resistance (Fig. S3E and Table S3). The *flp-1* promoter is active only in the two AVK interneurons (Greer et al., 2008). In addition, the *flp-1*, *tdc-1*, *glr-1*, and *glr-8* promoters drive expression in non-overlapping cells, except for the expression overlap in the two RIM interneurons by the *tdc-1* and *glr-1* promoters (Greer et al., 2008) (Fig. 3C). We refer to the sets of neurons where *flp-1*, *tdc-1*, *glr-1*, and *glr-8* are expressed as "DAF-1-sufficiency sets", because expression of *daf-1(+)* in any one of these sets of neurons is sufficient to lower the peroxide resistance of *daf-1* mutant nematodes. We conclude that DAF-1 functions redundantly in AVK interneurons and at least two other separate sets of neurons to lower the nematode's peroxide resistance.

Because during signal transduction the DAF-1/TGFβ-receptor inhibits the DAF-3/coSMAD transcription factor, DAF-3 should be active only in neurons where signaling through DAF-1 is inactive. As a result, we expected that when DAF-1 is active only in one DAF-1-sufficiency set of neurons, DAF-3 should be active only in neurons outside that set, including the neurons of other non-overlapping DAF-1-sufficiency sets. This implied that to increase peroxide resistance DAF-3 must be active in all DAF-1-sufficiency sets of neurons. To test this prediction, we examined the effect on peroxide resistance of restoring *daf-3(+)* expression in just one of the DAF-1-sufficiency sets of neurons in *daf-1; daf-3* double mutants. Confirming our prediction, we found that restoring *daf-3(+)* expression with the *tdc-1* promoter was not sufficient to increase peroxide resistance in *daf-1; daf-3* double mutants (Figs. 3K and S3F, and Table S3). In contrast, the peroxide resistance of *daf-1; daf-3* double mutants increased upon restoring *daf-3(+)* expression in all four DAF-1-sufficiency sets of neurons with a *daf-1* promoter (Fig. 3J and Table S3). We

conclude that the combination of the redundant action of DAF-1 in multiple sets of neurons and the repression of DAF-3 by DAF-1 in each of those neurons ensures that the nematode's peroxide resistance stays low until all DAF-1-sufficiency sets of neurons de-repress DAF-3/coSMAD (Fig. 3L). The way these neurons determine the nematode's peroxide resistance in response to DAF-7 signal levels is analogous to the way a logic NOR gate determines its output in response to its inputs. This circuit can be understood as an interneuron-consensus mechanism that ensures that target tissues induce a peroxide-protective response only if all DAF-1-sufficiency sets of neurons in the circuit fail to perceive the DAF-7 signal from ASI (Fig. 3M).

ASI regulates the nematode's peroxide resistance via a TGFβ-Insulin/IGF1 hormone relay

Previous studies have shown that distinct mechanisms act downstream of the DAF-3/coSMAD transcription factor to mediate the effects of DAF-7/TGFβ signaling on dauer-larva formation, fat storage, germline size, lifespan, and feeding (Dalfo et al., 2012; Greer et al., 2008; Shaw et al., 2007). Using a genetic approach, we asked whether DAF-7/TGFβ signaling acts via one or more of these mechanisms to regulate the nematode's peroxide resistance (Fig. 4A).

DAF-7 regulates dauer-larva formation via the nuclear hormone receptor DAF-12, which is the main switch driving the choice of reproductive growth or dauer arrest (Antebi et al., 2000). Loss of *daf-12* suppresses the constitutive dauer-formation phenotype of *daf-7* mutants during development (Thomas et al., 1993), but the *daf-12(rh61rh411)* null mutation did not suppress the increased peroxide resistance of *daf-7* mutant adults (Fig. 4B and Table S4). Therefore, DAF-7 regulates peroxide resistance and formation of peroxide-resistant dauer larvae via separate mechanisms.

The metabotropic glutamate receptors *mgl-1* and *mgl-3* are necessary for the increase in fat storage upon DAF-7-pathway inhibition (Greer et al., 2008). However, null mutations in either or both of these *mgl* genes did not affect peroxide resistance in *daf-1* mutants (Figs. 4C and S4, and Table S4). Thus, peroxide resistance and fat storage are also regulated via separate pathways downstream of DAF-1.

Germline size is reduced upon DAF-7-pathway inhibition (Dalfo et al., 2012). Genetic ablation of the germline increased the nematode's peroxide resistance by 57% compared to wild-type animals (Fig. 4D and Table S4), consistent with previous studies (Steinbaugh et al., 2015). However, *daf-1(m40)* increased peroxide resistance in both germline-ablated and germline-non-ablated nematodes (Fig. 4D and Table S4). In addition, *daf-3(mgDf90)* did not affect peroxide resistance in germline-ablated nematodes (Fig. 4E and Table S4). Therefore, DAF-1 regulates peroxide resistance via a germline-independent mechanism.

Last, DAF-7-pathway signaling lowers lifespan by promoting insulin/IGF1 receptor signaling (Shaw et al., 2007). Previous studies have shown that transcription of at least 11 of the 40 insulin/IGF1 genes in the genome is repressed by the DAF-3/coSMAD in response to lower levels of DAF-7 and DAF1 signaling (Liu et al., 2004; Narasimhan et al., 2011; Shaw et al., 2007). We found that deletion of the DAF-3-repressed insulin/IGF1 genes *ins-1, ins-3, ins-4, ins-5, ins-6,* or *daf-28* caused increases in peroxide resistance ranging between 11% and 65% (Figs. 5A, S5A, and S5B, and Table S5), suggesting DAF-7 lowers peroxide resistance by promoting signaling by the insulin/IGF1 receptor, DAF-2. The *daf-2(e1370)* strong loss-of-function mutation increased peroxide resistance about three-fold (Fig. 5B and Table S5), consistent with previous findings (Tullet et al., 2008). Double mutants of *daf-1(m40)* and *daf-2(e1370)* had higher peroxide resistance than the respective single mutants (Fig. 5B and Table S5), suggesting that the DAF-1 TGFβ receptor and the DAF-2 insulin/IGF1 receptor regulate

peroxide resistance via mechanisms that do not fully overlap. We considered the possibility that a DAF-2-dependent mechanism might mediate some of the effects of DAF-1 on peroxide resistance. If repressing the expression of insulin/IGF1 ligands of DAF-2 mediated part of the increased peroxide resistance of DAF-7-pathway inhibition, then one would expect the FOXO transcription factor DAF-16 to be necessary for those effects. DAF-16 is necessary for the increase in lifespan and most other phenotypes of mutants with reduced signaling by the DAF-2 insulin/IGF1 receptor (Kenyon et al., 1993; Lin et al., 1997; Ogg et al., 1997). We found that DAF-16 was also necessary for the increase in peroxide resistance of *daf-2(e1370)* mutants (Fig. 5C and Table S5) and for the increase in peroxide resistance of an *ins-4 ins-5 ins-6; daf-28* quadruple mutant (Fig. 5D and Table S5). The *daf-16(mu86)* null mutation decreased the peroxide resistance of *daf-7(e1372)* and *daf-1(m40)* mutants by nearly 50%, but caused only a small peroxide resistance reduction in wild-type nematodes (Figs. 5E and 5F, and Table S5). Therefore, regulation of peroxide resistance by the DAF-7/TGFβ signaling pathway is, in part, dependent on the DAF-16/FOXO transcription factor.

We examined whether other transcription factors might act with DAF-16 to increase peroxide resistance in *daf-1* mutants. Like DAF-16, the NRF orthologue SKN-1 and the TFEB orthologue HLH-30 are activated in response to reduced DAF-2 signaling (Lin et al., 2018; Tullet et al., 2008). The peroxide resistance of *daf-1(m40) hlh-30(tm1978)* double mutants was identical to that of *daf-1* single mutants (Fig. S5C and Table S5). Knockdown of *skn-1* via RNA interference (RNAi) decreased the peroxide resistance of *daf-1(m40)* mutants by 30% but did not affect peroxide resistance in wild-type nematodes (Fig. 5G and Table S5). RNAi of *skn-1* also decreased the peroxide resistance of *daf-16; daf-1* double mutants, suggesting that DAF-16 and SKN-1 functioned in a non-overlapping manner to promote peroxide resistance in *daf-1(m40)* mutants (Fig. 5H and Table S5). We propose that repression of insulin/IGF1 gene expression by DAF-3/coSMAD leads to a reduction in signaling by the DAF-2/insulin/IGF1 receptor, which

277 subsequently increases the nematode's peroxide resistance via transcriptional activation by
278 SKN-1/NRF and DAF-16/FOXO (Fig. 5N).
279
280 To identify which target tissues are important for increasing the nematode's peroxide resistance
281 via DAF-16 in response to reduced DAF-1 signaling, we determined the extent to which
282 restoring *daf-16(+)* expression in specific tissues using tissue-specific promoters increased the
283 peroxide resistance of *daf-16; daf-1* double mutants. As expected, peroxide resistance was
284 increased when we restored *daf-16(+)* expression with the endogenous *daf-16* promoter (Fig. 5I
285 and Table S5). Restoring *daf-16(+)* expression only in the intestine increased peroxide
286 resistance, albeit to a lesser extent than did re-expressing *daf-16(+)* with the endogenous *daf-*
287 *16* promoter (Fig. 5J and Table S5). Restoring *daf-16(+)* in neurons slightly increased peroxide
288 resistance (Fig. 5K), while restoring *daf-16(+)* in body-wall muscles had no effect (Fig. 5L and
289 Table S5). Restoring *daf-16(+)* expression in the hypodermis decreased peroxide resistance
290 slightly (Fig. 5M and Table S5); however, it is difficult to interpret these results because these
291 nematodes looked sickly (unlike *daf-1* and *daf-16* single and double mutants), consistent with
292 reports that selectively expressing *daf-16(+)* in the hypodermis was toxic (Libina et al., 2003).
293 Therefore, DAF-16/FOXO transcription in the intestine and neurons increases the nematode's
294 peroxide resistance when DAF-3/coSMAD is active due to reduced DAF-1 function (Fig. 5N).
295
296 **Food ingestion regulates the nematode's peroxide resistance via DAF-3/coSMAD**
297
298 Nematodes can be exposed directly to peroxides through food ingestion, and *daf-7* and *daf-1*
299 mutants have been shown to exhibit mild feeding defects (Greer et al., 2008). Therefore, we
300 considered the possibility that the increase in peroxide resistance of mutants with impaired
301 DAF-7-pathway signaling was due to their reduced feeding. Previous studies have shown that
302 the tyrosine decarboxylase TDC-1 and the tyramine β-hydroxylase TBH-1—biosynthetic

enzymes for the neurotransmitters tyramine and octopamine, respectively—are each necessary for the feeding defect of *daf-1* mutants as *daf-1;tdc-1* and *daf-1;tbh-1* double mutants have normal feeding behaviors (Greer et al., 2008). Surprisingly, despite restoring normal feeding to *daf-1* mutants, *tbh-1* and *tdc-1* null mutations did not suppress the increased peroxide resistance of *daf-1* mutants (Figs. 6A and S6A, and Table S6). In fact, both mutations further increased peroxide resistance in a *daf-1* mutant background. Because mutations that restored normal feeding to *daf-1* mutants increased the peroxide resistance of *daf-1* mutants, these findings suggested that the reduced feeding exhibited by *daf-1* mutants in fact reduces the magnitude of their increased peroxide resistance.

To investigate whether feeding has a direct effect on peroxide resistance, we first determined whether a wild-type nematode's feeding history (before peroxide exposure) might affect its subsequent peroxide resistance. We transferred nematodes to plates with different concentrations of *E. coli* for 24 hours prior to the start of the peroxide resistance assay and found that the *E. coli* concentration before the assay had a dose-dependent effect on peroxide resistance (Fig. 6B and Table S6). Animals grown on higher concentrations of *E. coli* had higher peroxide resistance. Strikingly, nematodes grown without *E. coli* for two days before the assay showed a six-fold decrease in peroxide resistance (Figs. 6C and S6B, and Table S6), even though they had access to plentiful *E. coli* during the assay.

Next, we tested whether reduced ingestion of *E. coli* was sufficient to mimic the effects of pre-exposure to reduced *E. coli* levels. Mutants in the pharyngeal-muscle specific nicotinic acetylcholine receptor subunit *eat-2* ingest bacteria more slowly due to reduced pharyngeal pumping (feeding) (Avery, 1993; Raizen et al., 1995). The *eat-2(ad1116)* loss-of-function mutation, which causes a strong feeding defect (Fig. 6E), decreased peroxide resistance by

25% relative to wild-type animals (Fig. 6D and Table S6). Therefore, impaired feeding leads to decreased peroxide resistance.

Finally, we asked whether feeding and DAF-7 signaling regulate peroxide resistance jointly, or independently. Unlike *eat-2* mutants, *daf-3* null single mutants did not decrease peroxide resistance compared with wild-type animals (Figs. 3A, 3B, and 6D). However, the *eat-2(ad1116)* mutation caused a larger decrease in peroxide resistance in *daf-3* mutants than in wild-type nematodes (Fig. 6D and Table S6), suggesting that *daf-3(+)* promotes peroxide resistance in *eat-2* mutants. This effect was not due to an enhancement of the feeding defect of *eat-2* mutants by the *daf-3* mutation, because *eat-2; daf-3* double mutants fed slightly more (not less) than *eat-2* single mutants (Fig. 6E). We propose that DAF-3 is activated in response to reduced feeding, leading to an increase in peroxide resistance. DAF-3 acts as an adaptive mechanism that partially offsets the detrimental effect of reduced feeding on peroxide resistance.

Taken together, these findings imply that both feeding on bacteria and DAF-3/coSMAD signaling increase peroxide resistance, but that they attenuate each other's effects (Fig. 6F). This cross-inhibition might enable nematodes to switch between DAF-3-dependent and DAF-3-independent mechanisms of peroxide resistance in response to changes in food ingestion and DAF-7 signal levels.

DAF-7/TGFβ signals that hydrogen-peroxide protection will be provided by catalases from *E. coli* and not by catalases from *C. elegans*

Why does DAF-7 from ASI function to decrease the nematode's peroxide resistance? ASI sensory neurons become active in response to perception of water-soluble signals from *E. coli* (Gallagher et al., 2013) and induce *daf-7* gene expression in a TAX-4-activity-dependent

manner (Chang et al., 2006). As a result, the ASI neurons upregulate *daf-7* expression in response to *E. coli* (Gallagher et al., 2013) and lower *daf-7* gene expression in response to starvation and low *E. coli* concentrations (Entchev et al., 2015; Ren et al., 1996). Lowering DAF-7 levels when *E. coli* is scarce may enable nematodes to prepare for a future of reduced feeding by attenuating the expected reduction in peroxide resistance caused by reduced feeding. But increasing DAF-7 levels when *E. coli* is abundant may render nematodes more vulnerable to peroxide. We reasoned that perhaps *C. elegans* decreases its own peroxide self-defenses via DAF-7 signaling from the ASI neurons when *E. coli* is abundant because *C. elegans* expects to be safe from peroxide attack in that setting.

To test that hypothesis, we first asked whether *E. coli* can protect nematodes from the lethal effects of peroxides. This required that we re-examine the conditions of the peroxide resistance assays, which were conducted using a lipid hydroperoxide (tert-butyl hydroperoxide, tBuOOH) widely used in *C. elegans* studies due to its stability (An et al., 2005). When we used hydrogen peroxide instead of tBuOOH, we could not kill *C. elegans* even with concentrations as high as 20 mM (Fig. 7A) which is well above the biologically plausible range of up to 3 mM hydrogen peroxide used by other bacteria to kill *C. elegans* (Bolm et al., 2004; Moy et al., 2004). This suggested that hydrogen peroxide, but not tBuOOH, was efficiently degraded by *E. coli*. This bacterium uses several scavenging systems to degrade hydrogen peroxide (Mishra and Imlay, 2012). The two *E. coli* catalases, KatG and KatE, are the predominant scavengers of hydrogen peroxide in the environment, and the peroxiredoxin, AhpCF, plays a minor role (Seaver and Imlay, 2001). *E. coli* JI377, a *KatG KatE AhpCF* triple null mutant strain which cannot scavenge any hydrogen peroxide from the environment (Seaver and Imlay, 2001), did not protect *C. elegans* from 1 mM hydrogen peroxide killing (Fig. 7B), whereas the *E. coli* MG1655 parental wild-type strain was protective (Fig. 7B). We propose that *E. coli* protects *C. elegans* from hydrogen-peroxide killing because it expresses catalases that efficiently deplete hydrogen

peroxide from the environment, creating a local environment where hydrogen peroxide is not a threat to *C. elegans*.

To determine whether DAF-7 regulates *C. elegans* hydrogen peroxide resistance, similar to its effects on tert-butyl hydroperoxide resistance, we examined resistance to hydrogen peroxide in *daf-7* mutants. In assays with the catalase mutant *E. coli* JI377 strain, we found that *daf-7(ok3125)* increased the nematode's hydrogen peroxide resistance over two-fold relative to wild-type nematodes (Figure 7B and Table S7). ASI-ablation also increased hydrogen peroxide resistance in assays with *E. coli* JI377 (Fig. S7A and Table S7). We propose that in response to TAX-4-dependent sensory perception of *E. coli*, the ASI sensory neurons express DAF-7/TGFβ to instruct target tissues to downregulate their hydrogen peroxide defenses.

Last, we investigated the possibility that reducing DAF-7-pathway signaling protects *C. elegans* from hydrogen-peroxide killing via a hydrogen-peroxide defense mechanism orthologous to the one by which *E. coli* protects *C. elegans*. The *C. elegans* genome contains three catalase genes in tandem—two-newly duplicated cytosolic catalases, *ctl-1* and *ctl-3*, and a peroxisomal catalase, *ctl-2*—which are the nematode orthologues of the two *E. coli* catalases, *KatG* and *KatE* (Petriv and Rachubinski, 2004). We expected the *C. elegans* catalase genes to be upregulated in response to reduced DAF-7 signaling, because all three catalase genes have DAF-16 and SKN-1 binding sites in their promoters (An and Blackwell, 2003; Park et al., 2009; Petriv and Rachubinski, 2004), and their mRNA and protein expression increase in a DAF-16-dependent manner when DAF-2 signaling is reduced (Dong et al., 2007; McElwee et al., 2003; Murphy et al., 2003). To determine whether endogenous catalases could protect *C. elegans* from hydrogen peroxide when *E. coli* is not able to deplete hydrogen peroxide from the environment, we examined the effects of simultaneously increasing the dosage of all three catalase genes. We found that *ctl-1/2/3* overexpression, which increases catalase activity ten-

406 fold (Doonan et al., 2008), more than doubled *C. elegans* hydrogen peroxide resistance in
407 assays with *E. coli* JI377 (Fig. 7C and Table S7). To investigate whether one of the endogenous
408 catalases might mediate the increased hydrogen peroxide resistance of nematodes with
409 reduced DAF-7-pathway signaling, we constructed double mutants between *daf-1* and individual
410 catalase genes. We found that the cytosolic catalase *ctl-1(ok1242)* null mutation abrogated
411 much of the increase in hydrogen peroxide resistance of *daf-1(m40)* mutants in assays with *E.*
412 *coli* JI377 (Fig. 7D and Table S7), but the peroxisomal catalase *ctl-2(ok1137)* null mutation did
413 not (Fig. S7B and Table S7). Therefore, the increase in hydrogen peroxide resistance of *daf-1*
414 mutants is mediated in part by the CTL-1 cytosolic catalase.
415
416 In line with this functional dependence, *ctl-1* mRNA levels were elevated up to two-fold in *daf-*
417 *7(ok3125)* and *daf-1(m40)* mutant adults grown on *E. coli* OP50 (Fig. 7E). This upregulation was
418 partially DAF-16-dependent, since the *daf-16(mu86)* mutation caused a small but statistically
419 significant reduction in *ctl-1* mRNA expression in *daf-1(m40)* mutants but not in wild-type
420 animals (Fig. 7E). The *ctl-1* gene product is expressed only in the intestine (Hamaguchi et al.,
421 2019), and this expression was elevated in *daf-1(m40)* mutants (Figs. 7F and 7G). Taken
422 together, these findings suggest that the DAF-7/TGFβ-pathway downregulates catalase gene
423 expression in the intestine, partly via DAF-16. We propose that DAF-7/TGFβ signaling enables
424 *C. elegans* to decide whether to induce its own hydrogen-peroxide degrading catalases or,
425 instead, freeload on protection provided by molecularly orthologous catalases from *E. coli* (Fig.
426 7H).
427
428
429 **Discussion**
430

Life forms throughout the evolutionary tree use hydrogen peroxide as an offensive weapon (Avery and Morgan, 1924; Imlay, 2018). Prevention and repair of the damage that hydrogen peroxide inflicts on macromolecules are critical for cellular health and survival (Chance et al., 1979). In this study, we found that in a simple animal, the nematode *C. elegans*, these protective responses are repressed in response to signals perceived by the nervous system. To our knowledge, the findings described here provide the first evidence of a multicellular organism modulating its defenses when it expects to freeload from the protection provided by molecularly orthologous defenses from individuals of a different species.

Signals from sensory neurons regulate *C. elegans* hydrogen peroxide defenses

We show here that sensory neurons regulate how long *C. elegans* nematodes can survive in the presence of peroxides in the environment. Peroxide resistance was higher in nematodes with a global impairment in sensory perception (Fig. 1A). Using a systematic neuron-specific genetic-ablation approach, we identified ten classes of sensory neurons that influence the nematode's peroxide resistance, including seven classes of neurons that normally decrease peroxide resistance and three classes of neurons that normally increase it (Fig. 1B). Why do so many neurons influence *C. elegans* peroxide resistance? One possibility is that these neurons respond to environments correlated with the threat of hydrogen peroxide.

Perception of water-soluble attractants by the amphid sensory neurons ASI, ASG, and ASK—neurons that when ablated caused some of the largest increases in peroxide resistance—helps *C. elegans* navigate towards bacteria (Bargmann and Horvitz, 1991a), its natural food source. We found that ingestion of *E. coli*, the nematode's food in laboratory experiments, increases *C. elegans* peroxide resistance (Fig. 6D). In addition, *E. coli* expresses scavenging enzymes that degrade hydrogen peroxide in the nematode's environment. These *E. coli* self-defense

457 mechanisms create a public good (West et al., 2006), an environment safe from the threat of
458 hydrogen peroxide, that benefits both *E. coli* and *C. elegans*. We propose that the control of
459 organismic peroxide resistance by neurons that sense bacteria enables nematodes to turn down
460 their peroxide self-defenses when they sense bacteria they deem protective. *C. elegans*
461 freeloads off the hydrogen peroxide self-defense mechanisms from *E. coli* (Fig. 7H), because it
462 uses a public good created by *E. coli*.
463
464 **The bacterial community influences the strategic choice between hydrogen peroxide**
465 **self-defense and freeloading**
466
467 We show here that *C. elegans* is safe from hydrogen peroxide attack when *E. coli* is abundant
468 because hydrogen-peroxide degrading enzymes from *E. coli* protect *C. elegans*. *E. coli*
469 degrades hydrogen peroxide in the environment primarily by expressing two catalases, KatG
470 and KatE, as these enzymes account for over 95% of *E. coli's* hydrogen-peroxide degrading
471 capacity (Seaver and Imlay, 2001). Catalase-positive *E. coli* can protect catalase-deficient *E.*
472 *coli* from hydrogen peroxide (Ma and Eaton, 1992). This facilitative relationship, where one
473 species creates an environment that promotes the survival of another (Bronstein, 2009), also
474 occurs across bacterial species in diverse environments: in dental plaque in the human mouth,
475 *Actinomyces naeslundii* protects catalase-deficient *Streptococcus gordonii* by removing
476 hydrogen peroxide (Jakubovics et al., 2008) and, in marine environments, catalase-positive
477 bacteria protect the catalase-deficient cyanobacterium *Prochlorococcus*, the major
478 photosynthetic organism in the open ocean (Zinser, 2018).
479
480 Unlike catalase-deficient bacteria receiving hydrogen-peroxide protection services from
481 surrounding bacteria, *C. elegans* is not catalase deficient. In *C. elegans*, TAX-4-dependent
482 sensory perception of *E. coli* stimulates the expression of DAF-7 in ASI (Chang et al., 2006;

Entchev et al., 2015; Gallagher et al., 2013; Ren et al., 1996). We found that when DAF-7 signaling is reduced, target tissues induce defense mechanisms that protect *C. elegans* from hydrogen peroxide. These mechanisms are mediated in part by the DAF-16-dependent expression in the intestine of the cytosolic catalase CTL-1. We propose that the TGFβ-insulin/IGF1 signaling hormonal relay that begins with DAF-7 secretion from ASI enables this sensory neuron to communicate to target tissues that they do not need to induce CTL-1 and other hydrogen-peroxide protection services because *E. coli* in the surrounding environment likely provide molecularly orthologous services. Thus, this sensory circuit enables nematodes to choose between hydrogen-peroxide self-defense and freeloading strategies (Fig. 7H).

Hydrogen peroxide is a threat to *C. elegans*. In its natural habitat of rotting fruits and vegetation, *C. elegans* encounters a wide variety of bacterial taxa (Samuel et al., 2016), and this community includes bacteria in many genera known to degrade or produce hydrogen peroxide (Passardi et al., 2007). Hydrogen peroxide produced by a bacterium from the *C. elegans* microbiome, *Rhizobium huautlense*, causes DNA damage to the nematodes (Kniazeva and Ruvkun, 2019), and many bacteria—including *S. pyogenes*, *S. pneumoniae*, *S. oralis*, and *E. faecium*—kill *C. elegans* by producing hydrogen peroxide, often in concentrations exceeding the 1 mM concentration present in our assays (Bolm et al., 2004; Jansen et al., 2002; Moy et al., 2004). *C. elegans* may also encounter hydrogen peroxide derived from fruits, leaves, and stems, because plants produce hydrogen peroxide to attack their pathogens (Arakawa et al., 2014; Daudi et al., 2012 ; Mehdy, 1994). *C. elegans* also induces production of hydrogen peroxide to attack its pathogens, including *E. faecalis* (Chavez et al., 2007). In this complex and variable habitat, deciding whether to induce hydrogen-peroxide defenses is challenging. *C. elegans* cells manage this challenge by relinquishing control of their cellular hydrogen-peroxide defenses to a neuronal circuit in the nematode's brain. This circuit might be able to integrate a wider variety of

inputs than individual cells could, enabling a better assessment of the threat of hydrogen peroxide and precise regulation of hydrogen-peroxide protective defenses.

Coordination of behavior, development, and physiology in response to the perceived threat of hydrogen peroxide

Assigning control of hydrogen peroxide cellular defenses to a sensory circuit in the brain could be beneficial because it enables *C. elegans* to avoid the energetic cost of unneeded protection. Tight control of hydrogen-peroxide defenses may also be necessary because a protective response might cause undesirable side effects. Nematodes overexpressing all three catalase genes exhibit a high level of mortality due to internal hatching of larvae, and this phenotype can be suppressed by joint overexpression of the superoxide dismutase SOD-1 (Doonan et al., 2008), an enzyme that produces hydrogen peroxide. While catalases can degrade large quantities of hydrogen peroxide, at low hydrogen peroxide concentrations these enzymes accumulate in the ferryl-radical intermediate of their catalytic cycle, which is a dangerous oxidizing agent (Imlay, 2013). Hydrogen peroxide is an important intracellular signaling molecule, and depletion of hydrogen peroxide by scavenging enzymes may interfere with signal transduction and affect cell behavior and differentiation (Veal et al., 2007).

Is the choice between hydrogen-peroxide self-defense and freeloading strategies regulated by DAF-7 limited to inducing hydrogen-peroxide protection services in target tissues? We favor an alternative possibility, that DAF-7 coordinates the induction of a broad phenotypic response to the perceived threat of hydrogen peroxide, because the phenotypic responses to lower DAF-7 signaling follow the expected desirable outcomes for animals that anticipate exposure to hydrogen peroxide: (i) re-routing development to form hydrogen-peroxide resistant dauer larva (Riddle and Albert, 1997); (ii) reducing proliferation of germline stem cells (Dalfo et al., 2012), to

prevent hydrogen-peroxide induced damage to their DNA (Wyatt et al., 2017; Zong et al., 2014), (iii) reducing oocyte fertilization and egg-laying (McKnight et al., 2014; Trent, 1982), to increase the chances of progeny survival; (iv) reducing feeding (Greer et al., 2008), since many pathogenic bacteria produce hydrogen peroxide; (v) avoiding high oxygen concentrations (Chang et al., 2006), which are oxidizing; and (vi) increasing the nematode's hydrogen peroxide resistance.

These diverse phenotypic responses might be triggered by different DAF-7 levels, reflecting the adaptive benefit of reducing the harm of hydrogen peroxide in each case. Perhaps for this reason, the DAF-7 signal is relayed via different circuits to target tissues mediating some of those responses. The DAF-1 receptor and the DAF-3/DAF-5 complex function in the somatic gonad to regulate germ-cell proliferation (Dalfo et al., 2012), and in RIM and RIC interneurons to regulate feeding, fat storage, egg laying, and dauer-larva formation (Greer et al., 2008). In contrast, to regulating hydrogen peroxide resistance, DAF-1 and DAF-3 function in at least three different sets of interneurons (Fig. 3L). One set includes RIM interneurons, and another comprises only the two AVK interneurons, which are not involved in regulating feeding, egg laying, and dauer-larva formation via DAF-1 signaling (Greer et al., 2008). The more complex role of interneuronal DAF-1 signaling in regulating hydrogen peroxide resistance suggests that *C. elegans* takes great care to avoid inducing hydrogen-peroxide protection services in target tissues unless DAF-7 levels are low.

When do animals choose between freeloading and self-defense strategies?

Our studies provide a template for understanding how complex animals coordinate cellular hydrogen-peroxide defenses. We identify sensory neurons that respond to bacterial cues as important regulators of hydrogen-peroxide protection by *C. elegans* target tissues. Similar

560 regulatory systems may exist in other animals. In mice, sensory neurons involved in pain
561 perception respond to cues from *Staphylococcus aureus* by releasing neuropeptides that inhibit
562 the activation of hydrogen-peroxide producing immune cells (Chiu et al., 2013), and some of the
563 neuropeptides secreted by these sensory neurons, including galanin and calcitonin gene-related
564 peptide, also induce hydrogen peroxide protection in target cells (Cui et al., 2010; Tullio et al.,
565 2017). Assigning control of cellular defenses to dedicated sensory circuits may represent a
566 general cellular-coordination tactic used by animals to regulate induction of self-defenses for
567 hydrogen peroxide and perhaps other threats.
568
569 We show that the two ASI amphid sensory neurons use a multistep signal relay to control the
570 extent to which target tissues protect *C. elegans* from hydrogen peroxide. The NOR circuit logic
571 implemented by these sequential hormonal steps may enable ASI to control the induction of a
572 sharp and specific peroxide-protective response in target tissues. In insects and mammals,
573 TGFβ and insulin/IGF1 signaling components regulate cellular antioxidant defenses (Brunet et
574 al., 2004; Clancy et al., 2001; Holzenberger et al., 2003; Kayanoki et al., 1994; Liu et al., 2012;
575 Tatar et al., 2003), so it will be interesting to determine if a conserved hormonal relay controls
576 hydrogen-peroxide defenses in all animals.
577
578 We delineate a neuronal circuit that processes sensory information to control the induction of
579 hydrogen peroxide protection services by *C. elegans* target tissues. In fluctuating environments,
580 we expect this circuit's output (self-defense or freeloading) to provide an evolutionarily optimal
581 strategy across its inputs (low or high *E. coli*) (Kussell and Leibler, 2005; Maynard Smith, 1982;
582 Wolf et al., 2005). While a freeloading strategy may provide maximum fitness by inactivating
583 self-defenses in environments where hydrogen peroxide is not a threat, this strategy need not
584 provide maximum health or longevity to the organism. Consistent with this, in addition to
585 lowering peroxide resistance in *C. elegans*, the ASI, ASG, and AWC amphid sensory neurons

586 also shorten this organism's lifespan in environments with no hydrogen peroxide (Alcedo and
587 Kenyon, 2004), and DAF-7/TGFβ signaling from ASI also shortens *C. elegans* lifespan in those
588 environments (Shaw et al., 2007). Thus, inducing latent self-defenses in environments where
589 they are normally not induced can provide an approach to increase longevity in *C. elegans*.
590 Because sensory perception and catalases also determine health and longevity in invertebrate
591 and vertebrate animals (Apfeld and Kenyon, 1999; Libert et al., 2007; Murphy et al., 2007;
592 Perez-Estrada et al., 2019; Riera et al., 2014), it is likely that sensory modulation presents a
593 promising approach to induce latent defenses that could increase health and longevity in all
594 animals.
595
596
597 **Materials and Methods**
598
599 ***C. elegans* culture, strains, and transgenes**
600
601 Wild-type *C. elegans* was Bristol N2. *C. elegans* were cultured on NGM agar plates seeded with
602 *E. coli* OP50, unless noted otherwise. For a list of all bacterial and worm strains used in this
603 study, see Table S8 and Table S9, respectively. Double and triple mutant worms were
604 generated by standard genetic methods. For a list of PCR genotyping primers and enzymes,
605 and phenotypes used for strain construction, see Table S10. The *Ptdc-1::daf-3(+)::GFP*
606 (pKA533) and *Pdaf-1::daf-3(+)::GFP* (pKA534) plasmids (kindly provided by Kaveh Ashrafi)
607 were injected at 30 ng/µl into *daf-1(m40) IV*; *daf-3(mgDf90) X* with 20 ng/µl *Pmyo-2::RFP* and
608 20 ng/µl *Punc-122::DsRed*, respectively, as co-injection markers.
609
610 **Survival assays**
611

612 Automated survival assays were conducted using a *C. elegans* lifespan machine scanner
613 cluster (Stroustrup et al., 2013). This platform enables the acquisition of survival curves with
614 very high temporal resolution and large population sizes. All chemicals were obtained from
615 Sigma. For hydrogen peroxide, tert-butyl hydroperoxide, sodium arsenite, paraquat, and
616 dithiothreitol assays, the compound was added to molten agar immediately before pouring onto
617 50 mm NGM agar plates. Plates were dried (Stroustrup et al., 2013) and seeded with 100 µl of
618 concentrated *E. coli* OP50 resuspended at an OD_{600} of 20 (Entchev et al., 2015). For RNAi
619 experiments, the appropriate *E. coli* HT115 (DE3) strain was used instead. For hydrogen
620 peroxide assays, *E. coli* MG1655 or JI377 were used instead (Seaver and Imlay, 2001).
621 Nematodes were cultured at 20°C until the onset of adulthood, and then cultured at 25°C—to
622 potentially enhance *daf-7* mutant phenotypes (Ren et al., 1996; Shaw et al., 2007)—in groups of
623 up to 100, on plates with 10 µg/ml 5-fluoro-2-deoxyuridine (FUDR), to avoid vulval rupture
624 (Leiser et al., 2016), prevent matricidal effects of *daf-7* pathway mutants (Shaw et al., 2007),
625 and eliminate live progeny. As an alternative to FUDR, we inhibited formation of the eggshell of
626 fertilized *C. elegans* embryos with RNAi of *egg-5* (Entchev et al., 2015), with identical results
627 (Fig. S2A and S2C-D, and Table S2). For sodium arsenite, paraquat, and DTT assays, we
628 adjusted the concentrations of these compounds to reduce the survival of wild-type nematodes
629 about as much as in the peroxide survival assays. For experiments with *daf-1; daf-2* double
630 mutants, which only develop as dauers at 20°C, all strains were grown at 15°C instead of 20°C
631 until the onset of adulthood. For food-conditioning experiments, *E. coli* OP50 was resuspended
632 in S Basal containing streptomycin (50 µg/ml) and seeded onto plates supplemented with both
633 streptomycin and carbenicillin, each at 50 µg/ml, as described (Entchev et al., 2015). For *daf-1*,
634 *daf-3*, and *daf-16* transgenic-rescue experiments, we picked only nematodes exhibiting bright
635 expression of the respective GFP-fusion proteins. Day 2 adults were transferred to lifespan
636 machine assay plates. A typical experiment consisted of up to four genotypes or conditions, with
637 4 assay plates of each genotype or condition, each assay plate containing a maximum of 40

638 nematodes, and 16 assay plates housed in the same scanner. All experiments were repeated at
639 least once, yielding the same results. Scanner temperature was calibrated to 25°C with a
640 thermocouple (ThermoWorks USB-REF) on the bottom of an empty assay plate. Death times
641 were automatically detected by the lifespan machine's image-analysis pipeline, with manual
642 curation of each death time through visual inspection of all collected image data (Stroustrup et
643 al., 2013), without knowledge of genotype or experimental condition.
644
645 **RNA interference**
646
647 *E. coli* HT115 (DE3) bacteria with plasmids expressing dsRNA targeting specific genes were
648 obtained from the Ahringer and Vidal libraries (Kamath et al., 2001; Rual et al., 2004). Empty
649 vector plasmid pL4440 was used as control. Bacterial cultures were grown in LB broth with 100
650 µg/ml ampicillin at 37°C, induced with 0.1 M isopropyl-thiogalactopyranoside (IPTG) at 37°C for
651 4 hours, concentrated to an OD_{600} of 20, and seeded onto NGM agar plates containing 50 µg/ml
652 carbenicillin and 2 mM IPTG.
653
654 **Quantitative RT-PCR**
655
656 Total RNA was extracted from day 2 animals that were transferred at the L4 stage onto NGM
657 agar plates with 10 µg/ml FUDR seeded with *E. coli* OP50 and grown at 25ºC. RNA extraction
658 and cDNA preparation were performed as described (Amrit et al., 2019). Quantitative RT-PCRs
659 were performed using the Biorad CFX Connect machine. PCR reactions were undertaken in 96-
660 well optical reaction plates (Bio-Rad Hard Shell PCR Plates). A 20 µl PCR reaction was set up
661 in each well using the SYBR PowerUp Green Master Mix (Applied Biosystems, USA) with 10ng
662 of the converted cDNA and 0.3 M primers. For each gene at least three independent biological
663 samples were tested, each with three technical replicates. Primers used in this study include

664 TTCCATTTCAAGCCTGCTC (*ctl-1* Fwd), ATAGTCTGGATCCGAAGAGG (*ctl-1* Rev),
665 GGATTTGGACATGCTCCTC (*rpl-32* Fwd) (Amrit et al., 2019), and GATTCCCTTGCGGCTCTT
666 (*rpl-32* Rev) (Amrit et al., 2019).
667
668 **Microscopy**
669
670 Transgenic animals expressing a Bxy-CTL-1::GFP fusion under the control of the *C. elegans ctl-*
671 *1* promoter (Hamaguchi et al., 2019) were scored at the young-adult stage using a fluorescence
672 dissection stereomicroscope (Zeiss Discovery V12) under 100x magnification, following a
673 scheme previously used to score a *gcs-1p::GFP* reporter with a similar pattern of intestinal
674 expression (Wang et al., 2010). Low: only anterior or posterior intestine with patches of GFP.
675 Medium: anterior and posterior intestine with patches GFP, middle of the intestine with dim
676 GFP. High: anterior and posterior intestine with non-patchy GFP expression, middle of the
677 intestine with patchy or dim GFP. Very high: strong and non-patchy GFP expression throughout
678 the intestine. Fluorescence imaging was conducted as previously described (Romero-Aristizabal
679 et al., 2014) with an Axioskop 2 FS plus microscope (Zeiss) equipped with a D470/20x
680 excitation filter, a 500dcxr dichroic mirror, and a HQ535/50m emission filter (all from Chroma),
681 using a Plan-Apochromat 10X 0.45 NA 2 mm working distance objective lens (1063-139, Zeiss).
682 Young adult worms were placed on petri plates with modified Nematode Growth Media (to
683 minimize background fluorescence) containing 6 mM levamisole to immobilize the animals
684 (Romero-Aristizabal et al., 2014). Images were acquired with a Cool SNAP HQ^2 14-bit camera
685 (Photometrics) at 4x4 binning and 20 ms exposure. We performed background subtraction by
686 removing the mode intensity value of the entire image from each pixel. This procedure removes
687 the background due to the agar and the camera noise, since most pixels in our images were
688 part of the background. All microscopy was performed at 22°C.
689

690 **Behavioral assays**

691

692 Pharyngeal pumping was assayed for 30 seconds on day 2 adults at 25°C using a dissecting
693 microscope under 100x magnification.

694

695 **Statistical analysis**

696

697 All statistical analyses were performed in JMP Pro version 14 (SAS). Survival curves were
698 calculated using the Kaplan-Meier method. We used the log-rank test to determine if the
699 survival functions of two or more groups were equal. For pumping-period assays, we used the
700 Tukey HSD post-hoc test to determine which pairs of groups in the sample differ. For intestinal
701 GFP expression assays, we used ordinal logistic regression to determine if expression levels
702 were equal between groups.

703

704

705 **Acknowledgements**

706

707 We thank Jennifer Whangbo, Phyllis Strauss, Veronica Godoy, and Erin Cram for critical
708 reading and detailed comments on our manuscript. Joy Alcedo, Kaveh Ashrafi, Ryan Baugh,
709 Denise Ferkey, Takaaki Hirotsu, James Imlay, Koichi Hasegawa, Jane Hubbard, Charlotte
710 Kelley, Dennis Kim, Junho Lee, Andres Maricq, Roger Pocock, Piali Sengupta, Young-Jai You,
711 and Yun Zhang kindly provided strains and plasmids. We benefitted from discussions with
712 members of Erin Cram's lab, Veronica Godoy, Edward Geisinger, and Yunrong Chai. Some
713 strains were provided by the CGC, which is funded by NIH Office of Research Infrastructure
714 Programs (P40 OD010440), and the National BioResources Project, Japan. The research was

715 supported by National Science Foundation CAREER grant 1750065 to J.A. and National
716 Institutes of Health grant R01AG051659 to A.G.

717

718

719 **Author contributions**

720

721 J.S., F.S., W.H. and J.A. conceived and designed experiments, and analyzed data. J.S., F.S.,
722 S.S., S.J., J.S., H.T., S.B., N.Mc., A.V., and W.S. constructed strains and performed
723 experiments. F.A performed Q-PCR experiments. J.A and A.G. provided guidance. J.S., F.S.,
724 and J.A. interpreted results and wrote the manuscript with contributions from the other authors.

725

726

727 **Competing interests**

728

729 The authors declare that no competing interests exist.

730

731

732 **References**

733 Alcedo, J., and Kenyon, C. (2004). Regulation of C. elegans Longevity by Specific Gustatory
734 and Olfactory Neurons. Neuron *41*, 45-55.

735 Amrit, F.R.G., Naim, N., Ratnappan, R., Loose, J., Mason, C., Steenberge, L., McClendon, B.T.,
736 Wang, G., Driscoll, M., Yanowitz, J.L.*, et al.* (2019). The longevity-promoting factor, TCER-1,
737 widely represses stress resistance and innate immunity. Nature communications *10*, 3042.

738 An, J.H., and Blackwell, T.K. (2003). SKN-1 links C. elegans mesendodermal specification to a
739 conserved oxidative stress response. Genes & development *17*, 1882-1893.

740 An, J.H., Vranas, K., Lucke, M., Inoue, H., Hisamoto, N., Matsumoto, K., and Blackwell, T.K.
741 (2005). Regulation of the Caenorhabditis elegans oxidative stress defense protein SKN-1 by
742 glycogen synthase kinase-3. Proc Natl Acad Sci U S A *102*, 16275-16280.

743 Antebi, A., Yeh, W.H., Tait, D., Hedgecock, E.M., and Riddle, D.L. (2000). daf-12 encodes a
744 nuclear receptor that regulates the dauer diapause and developmental age in C. elegans.
745 Genes & development *14*, 1512-1527.

746 Apfeld, J., and Kenyon, C. (1999). Regulation of lifespan by sensory perception in
747 Caenorhabditis elegans. Nature *402*, 804-809.

748 Arakawa, H., Takasaki, M., Tajima, N., Fukamachi, H., and Igarashi, T. (2014). Antibacterial
749 activities of persimmon extracts relate with their hydrogen peroxide concentration. Biological &
750 pharmaceutical bulletin *37*, 1119-1123.

751 Avery, L. (1993). The genetics of feeding in Caenorhabditis elegans. Genetics *133*, 897-917.

752 Avery, O.T., and Morgan, H.J. (1924). The Occurrence of Peroxide in Cultures of
753 Pneumococcus. The Journal of experimental medicine *39*, 275-287.

754 Bargmann, C.I., and Horvitz, H.R. (1991a). Chemosensory neurons with overlapping functions
755 direct chemotaxis to multiple chemicals in C. elegans. Neuron *7*, 729-742.

756 Bargmann, C.I., and Horvitz, H.R. (1991b). Control of larval development by chemosensory
757 neurons in Caenorhabditis elegans. Science *251*, 1243-1246.

758 Bolm, M., Jansen, W.T., Schnabel, R., and Chhatwal, G.S. (2004). Hydrogen peroxide-mediated
759 killing of Caenorhabditis elegans: a common feature of different streptococcal species. Infection
760 and immunity *72*, 1192-1194.

761 Bronstein, J.L. (2009). The evolution of facilitation and mutualism. J Ecol *97*, 1160-1170.

762 Brunet, A., Sweeney, L.B., Sturgill, J.F., Chua, K.F., Greer, P.L., Lin, Y., Tran, H., Ross, S.E.,
763 Mostoslavsky, R., Cohen, H.Y.*, et al.* (2004). Stress-dependent regulation of FOXO transcription
764 factors by the SIRT1 deacetylase. Science *303*, 2011-2015.

765 Chalfie, M., Sulston, J.E., White, J.G., Southgate, E., Thomson, J.N., and Brenner, S. (1985).
766 The neural circuit for touch sensitivity in Caenorhabditis elegans. The Journal of neuroscience :
767 the official journal of the Society for Neuroscience *5*, 956-964.

768 Chance, B., Sies, H., and Boveris, A. (1979). Hydroperoxide metabolism in mammalian organs.
769 Physiological reviews *59*, 527-605.

770 Chang, A.J., Chronis, N., Karow, D.S., Marletta, M.A., and Bargmann, C.I. (2006). A distributed
771 chemosensory circuit for oxygen preference in C. elegans. PLoS Biol *4*, e274.

772 Chang, S., Johnston, R.J., Jr., and Hobert, O. (2003). A transcriptional regulatory cascade that
773 controls left/right asymmetry in chemosensory neurons of C. elegans. Genes & development *17*,
774 2123-2137.

775 Chavez, V., Mohri-Shiomi, A., Maadani, A., Vega, L.A., and Garsin, D.A. (2007). Oxidative
776 stress enzymes are required for DAF-16-mediated immunity due to generation of reactive
777 oxygen species by Caenorhabditis elegans. Genetics *176*, 1567-1577.

778 Chelur, D.S., and Chalfie, M. (2007). Targeted cell killing by reconstituted caspases. Proc Natl
779 Acad Sci U S A *104*, 2283-2288.

780 Chiu, I.M., Heesters, B.A., Ghasemlou, N., Von Hehn, C.A., Zhao, F., Tran, J., Wainger, B.,
781 Strominger, A., Muralidharan, S., Horswill, A.R.*, et al.* (2013). Bacteria activate sensory neurons
782 that modulate pain and inflammation. Nature *501*, 52-57.

783 Clancy, D.J., Gems, D., Harshman, L.G., Oldham, S., Stocker, H., Hafen, E., Leevers, S.J., and
784 Partridge, L. (2001). Extension of life-span by loss of CHICO, a Drosophila insulin receptor
785 substrate protein. Science *292*, 104-106.

786 Coburn, C.M., and Bargmann, C.I. (1996). A putative cyclic nucleotide-gated channel is required
787 for sensory development and function in C. elegans. Neuron *17*, 695-706.

788 Cui, J., Chen, Q., Yue, X., Jiang, X., Gao, G.F., Yu, L.C., and Zhang, Y. (2010). Galanin
789 protects against intracellular amyloid toxicity in human primary neurons. Journal of Alzheimer's
790 disease : JAD *19*, 529-544.

791 da Graca, L.S., Zimmerman, K.K., Mitchell, M.C., Kozhan-Gorodetska, M., Sekiewicz, K.,
792 Morales, Y., and Patterson, G.I. (2004). DAF-5 is a Ski oncoprotein homolog that functions in a
793 neuronal TGF beta pathway to regulate C. elegans dauer development. Development *131*, 435-
794 446.

795 Dalfo, D., Michaelson, D., and Hubbard, E.J. (2012). Sensory regulation of the C. elegans
796 germline through TGF-beta-dependent signaling in the niche. Curr Biol *22*, 712-719.

797 Daudi, A., Cheng, Z., O'Brien, J.A., Mammarella, N., Khan, S., Ausubel, F.M., and Bolwell, G.P.
798 (2012). The apoplastic oxidative burst peroxidase in Arabidopsis is a major component of
799 pattern-triggered immunity. The Plant cell *24*, 275-287.

800 Dong, M.Q., Venable, J.D., Au, N., Xu, T., Park, S.K., Cociorva, D., Johnson, J.R., Dillin, A., and
801 Yates, J.R., 3rd (2007). Quantitative mass spectrometry identifies insulin signaling targets in C.
802 elegans. Science *317*, 660-663.

803 Doonan, R., McElwee, J.J., Matthijssens, F., Walker, G.A., Houthoofd, K., Back, P., Matscheski,
804 A., Vanfleteren, J.R., and Gems, D. (2008). Against the oxidative damage theory of aging:
805 superoxide dismutases protect against oxidative stress but have little or no effect on life span in
806 Caenorhabditis elegans. Genes & development *22*, 3236-3241.

807 Entchev, E.V., Patel, D.S., Zhan, M., Steele, A.J., Lu, H., and Ch'ng, Q. (2015). A gene-
808 expression-based neural code for food abundance that modulates lifespan. eLife *4*, e06259.

809 Gallagher, T., Kim, J., Oldenbroek, M., Kerr, R., and You, Y.J. (2013). ASI regulates satiety
810 quiescence in C. elegans. The Journal of neuroscience : the official journal of the Society for
811 Neuroscience *33*, 9716-9724.

812 Georgi, L.L., Albert, P.S., and Riddle, D.L. (1990). daf-1, a C. elegans gene controlling dauer
813 larva development, encodes a novel receptor protein kinase. Cell *61*, 635-645.

814 Gray, J.M., Karow, D.S., Lu, H., Chang, A.J., Chang, J.S., Ellis, R.E., Marletta, M.A., and
815 Bargmann, C.I. (2004). Oxygen sensation and social feeding mediated by a C. elegans
816 guanylate cyclase homologue. Nature *430*, 317-322.

817 Greer, E.R., Perez, C.L., Van Gilst, M.R., Lee, B.H., and Ashrafi, K. (2008). Neural and
818 molecular dissection of a C. elegans sensory circuit that regulates fat and feeding. Cell Metab *8*,
819 118-131.

820 Gunther, C.V., Georgi, L.L., and Riddle, D.L. (2000). A Caenorhabditis elegans type I TGF beta
821 receptor can function in the absence of type II kinase to promote larval development.
822 Development *127*, 3337-3347.

823 Hamaguchi, T., Sato, K., Vicente, C.S.L., and Hasegawa, K. (2019). Nematicidal actions of the
824 marigold exudate alpha-terthienyl: oxidative stress-inducing compound penetrates nematode
825 hypodermis. Biol Open *8*.

826 Holzenberger, M., Dupont, J., Ducos, B., Leneuve, P., Geloen, A., Even, P.C., Cervera, P., and
827 Le Bouc, Y. (2003). IGF-1 receptor regulates lifespan and resistance to oxidative stress in mice.
828 Nature *421*, 182-187.

829 Imlay, J.A. (2013). The molecular mechanisms and physiological consequences of oxidative
830 stress: lessons from a model bacterium. Nature reviews Microbiology *11*, 443-454.

831 Imlay, J.A. (2018). Where in the world do bacteria experience oxidative stress? Environmental
832 microbiology.

833 Jakubovics, N.S., Gill, S.R., Vickerman, M.M., and Kolenbrander, P.E. (2008). Role of hydrogen
834 peroxide in competition and cooperation between Streptococcus gordonii and Actinomyces
835 naeslundii. FEMS microbiology ecology *66*, 637-644.

836 Jansen, W.T., Bolm, M., Balling, R., Chhatwal, G.S., and Schnabel, R. (2002). Hydrogen
837 peroxide-mediated killing of Caenorhabditis elegans by Streptococcus pyogenes. Infection and
838 immunity *70*, 5202-5207.

839 Kamath, R.S., Martinez-Campos, M., Zipperlen, P., Fraser, A.G., and Ahringer, J. (2001).
840 Effectiveness of specific RNA-mediated interference through ingested double-stranded RNA in
841 Caenorhabditis elegans. Genome Biol *2*, research2.1-2.10.

842 Kaplan, H.S., Nichols, A.L.A., and Zimmer, M. (2018). Sensorimotor integration in
843 Caenorhabditis elegans: a reappraisal towards dynamic and distributed computations.
844 Philosophical transactions of the Royal Society of London Series B, Biological sciences *373*.

845 Kayanoki, Y., Fujii, J., Suzuki, K., Kawata, S., Matsuzawa, Y., and Taniguchi, N. (1994).
846 Suppression of antioxidative enzyme expression by transforming growth factor-beta 1 in rat
847 hepatocytes. J Biol Chem *269*, 15488-15492.

848 Kenyon, C., Chang, J., Gensch, E., Rudner, A., and Tabtiang, R. (1993). A C. elegans mutant
849 that lives twice as long as wild type. Nature *366*, 461-464.

850 Kniazeva, M., and Ruvkun, G. (2019). Rhizobium induces DNA damage in Caenorhabditis
851 elegans intestinal cells. Proc Natl Acad Sci U S A *116*, 3784-3792.

852 Komatsu, H., Mori, I., Rhee, J.S., Akaike, N., and Ohshima, Y. (1996). Mutations in a cyclic
853 nucleotide-gated channel lead to abnormal thermosensation and chemosensation in C. elegans.
854 Neuron *17*, 707-718.

855 Kussell, E., and Leibler, S. (2005). Phenotypic diversity, population growth, and information in
856 fluctuating environments. Science *309*, 2075-2078.

857 Leiser, S.F., Jafari, G., Primitivo, M., Sutphin, G.L., Dong, J., Leonard, A., Fletcher, M., and
858 Kaeberlein, M. (2016). Age-associated vulval integrity is an important marker of nematode
859 healthspan. Age *38*, 419-431.

860 Libert, S., Zwiener, J., Chu, X., Vanvoorhies, W., Roman, G., and Pletcher, S.D. (2007).
861 Regulation of Drosophila life span by olfaction and food-derived odors. Science *315*, 1133-1137.

862 Libina, N., Berman, J.R., and Kenyon, C. (2003). Tissue-specific activities of C. elegans DAF-16
863 in the regulation of lifespan. Cell *115*, 489-502.

Lin, K., Dorman, J.B., Rodan, A., and Kenyon, C. (1997). daf-16: An HNF-3/forkhead family member that can function to double the life-span of Caenorhabditis elegans. Science *278*, 1319-1322.

Lin, X.X., Sen, I., Janssens, G.E., Zhou, X., Fonslow, B.R., Edgar, D., Stroustrup, N., Swoboda, P., Yates, J.R., 3rd, Ruvkun, G.*, et al.* (2018). DAF-16/FOXO and HLH-30/TFEB function as combinatorial transcription factors to promote stress resistance and longevity. Nature communications *9*, 4400.

Liu, R.M., Vayalil, P.K., Ballinger, C., Dickinson, D.A., Huang, W.T., Wang, S., Kavanagh, T.J., Matthews, Q.L., and Postlethwait, E.M. (2012). Transforming growth factor beta suppresses glutamate-cysteine ligase gene expression and induces oxidative stress in a lung fibrosis model. Free Radic Biol Med *53*, 554-563.

Liu, T., Zimmerman, K.K., and Patterson, G.I. (2004). Regulation of signaling genes by TGFbeta during entry into dauer diapause in C. elegans. BMC developmental biology *4*, 11.

Ma, M., and Eaton, J.W. (1992). Multicellular oxidant defense in unicellular organisms. Proc Natl Acad Sci U S A *89*, 7924-7928.

Mak, H.Y., Nelson, L.S., Basson, M., Johnson, C.D., and Ruvkun, G. (2006). Polygenic control of Caenorhabditis elegans fat storage. Nature genetics *38*, 363-368.

Maynard Smith, J. (1982). Evolution and the theory of games (Cambridge ; New York: Cambridge University Press).

McElwee, J., Bubb, K., and Thomas, J.H. (2003). Transcriptional outputs of the Caenorhabditis elegans forkhead protein DAF-16. Aging Cell *2*, 111-121.

McKnight, K., Hoang, H.D., Prasain, J.K., Brown, N., Vibbert, J., Hollister, K.A., Moore, R., Ragains, J.R., Reese, J., and Miller, M.A. (2014). Neurosensory perception of environmental cues modulates sperm motility critical for fertilization. Science *344*, 754-757.

Mehdy, M.C. (1994). Active Oxygen Species in Plant Defense against Pathogens. Plant Physiol *105*, 467-472.

Meisel, J.D., Panda, O., Mahanti, P., Schroeder, F.C., and Kim, D.H. (2014). Chemosensation of bacterial secondary metabolites modulates neuroendocrine signaling and behavior of C. elegans. Cell *159*, 267-280.

Mishra, S., and Imlay, J. (2012). Why do bacteria use so many enzymes to scavenge hydrogen peroxide? Archives of biochemistry and biophysics *525*, 145-160.

Mori, I., and Ohshima, Y. (1995). Neural regulation of thermotaxis in Caenorhabditis elegans. Nature *376*, 344-348.

Moy, T.I., Mylonakis, E., Calderwood, S.B., and Ausubel, F.M. (2004). Cytotoxicity of hydrogen peroxide produced by Enterococcus faecium. Infection and immunity *72*, 4512-4520.

Murphy, C.T., Lee, S.J., and Kenyon, C. (2007). Tissue entrainment by feedback regulation of insulin gene expression in the endoderm of Caenorhabditis elegans. Proc Natl Acad Sci U S A *104*, 19046-19050.

Murphy, C.T., McCarroll, S.A., Bargmann, C.I., Fraser, A., Kamath, R.S., Ahringer, J., Li, H., and Kenyon, C. (2003). Genes that act downstream of DAF-16 to influence the lifespan of Caenorhabditis elegans. Nature *424*, 277-283.

905 Narasimhan, S.D., Yen, K., Bansal, A., Kwon, E.S., Padmanabhan, S., and Tissenbaum, H.A.
906 (2011). PDP-1 links the TGF-beta and IIS pathways to regulate longevity, development, and
907 metabolism. PLoS genetics *7*, e1001377.

908 Ogg, S., Paradis, S., Gottlieb, S., Patterson, G.I., Lee, L., Tissenbaum, H.A., and Ruvkun, G.
909 (1997). The Fork head transcription factor DAF-16 transduces insulin-like metabolic and
910 longevity signals in C. elegans. Nature *389*, 994-999.

911 Park, S.K., Tedesco, P.M., and Johnson, T.E. (2009). Oxidative stress and longevity in
912 Caenorhabditis elegans as mediated by SKN-1. Aging Cell *8*, 258-269.

913 Passardi, F., Zamocky, M., Favet, J., Jakopitsch, C., Penel, C., Obinger, C., and Dunand, C.
914 (2007). Phylogenetic distribution of catalase-peroxidases: are there patches of order in chaos?
915 Gene *397*, 101-113.

916 Patterson, G.I., Koweek, A., Wong, A., Liu, Y., and Ruvkun, G. (1997). The DAF-3 Smad protein
917 antagonizes TGF-beta-related receptor signaling in the Caenorhabditis elegans dauer pathway.
918 Genes & development *11*, 2679-2690.

919 Perez-Estrada, J.R., Hernandez-Garcia, D., Leyva-Castro, F., Ramos-Leon, J., Cuevas-Benitez,
920 O., Diaz-Munoz, M., Castro-Obregon, S., Ramirez-Solis, R., Garcia, C., and Covarrubias, L.
921 (2019). Reduced lifespan of mice lacking catalase correlates with altered lipid metabolism
922 without oxidative damage or premature aging. Free Radic Biol Med *135*, 102-115.

923 Perkins, L.A., Hedgecock, E.M., Thomson, J.N., and Culotti, J.G. (1986). Mutant sensory cilia in
924 the nematode Caenorhabditis elegans. Developmental biology *117*, 456-487.

925 Petriv, O.I., and Rachubinski, R.A. (2004). Lack of peroxisomal catalase causes a progeric
926 phenotype in Caenorhabditis elegans. J Biol Chem *279*, 19996-20001.

927 Prahlad, V., Cornelius, T., and Morimoto, R.I. (2008). Regulation of the cellular heat shock
928 response in Caenorhabditis elegans by thermosensory neurons. Science *320*, 811-814.

929 Raizen, D.M., Lee, R.Y., and Avery, L. (1995). Interacting genes required for pharyngeal
930 excitation by motor neuron MC in Caenorhabditis elegans. Genetics *141*, 1365-1382.

931 Ren, P., Lim, C.S., Johnsen, R., Albert, P.S., Pilgrim, D., and Riddle, D.L. (1996). Control of C.
932 elegans larval development by neuronal expression of a TGF-beta homolog. Science *274*,
933 1389-1391.

934 Riddle, D.L., and Albert, P.S. (1997). Regulation of Dauer Larva Development. In C elegans II
935 (Plainview, N.Y.: Cold Spring Harbor Laboratory Press), pp. 739-768.

936 Riera, C.E., Huising, M.O., Follett, P., Leblanc, M., Halloran, J., Van Andel, R., de Magalhaes
937 Filho, C.D., Merkwirth, C., and Dillin, A. (2014). TRPV1 pain receptors regulate longevity and
938 metabolism by neuropeptide signaling. Cell *157*, 1023-1036.

939 Romero-Aristizabal, C., Marks, D.S., Fontana, W., and Apfeld, J. (2014). Regulated spatial
940 organization and sensitivity of cytosolic protein oxidation in Caenorhabditis elegans. Nature
941 communications *5*, 5020.

942 Rual, J.F., Ceron, J., Koreth, J., Hao, T., Nicot, A.S., Hirozane-Kishikawa, T., Vandenhaute, J.,
943 Orkin, S.H., Hill, D.E., van den Heuvel, S.*, et al.* (2004). Toward improving Caenorhabditis
944 elegans phenome mapping with an ORFeome-based RNAi library. Genome research *14*, 2162-
945 2168.

946 Samuel, B.S., Rowedder, H., Braendle, C., Felix, M.A., and Ruvkun, G. (2016). Caenorhabditis
947 elegans responses to bacteria from its natural habitats. Proc Natl Acad Sci U S A *113*, E3941-
948 3949.

949 Seaver, L.C., and Imlay, J.A. (2001). Alkyl hydroperoxide reductase is the primary scavenger of
950 endogenous hydrogen peroxide in Escherichia coli. Journal of bacteriology *183*, 7173-7181.

951 Shaw, W.M., Luo, S., Landis, J., Ashraf, J., and Murphy, C.T. (2007). The C. elegans TGF-beta
952 Dauer pathway regulates longevity via insulin signaling. Curr Biol *17*, 1635-1645.

953 Steinbaugh, M.J., Narasimhan, S.D., Robida-Stubbs, S., Moronetti Mazzeo, L.E., Dreyfuss,
954 J.M., Hourihan, J.M., Raghavan, P., Operana, T.N., Esmaillie, R., and Blackwell, T.K. (2015).
955 Lipid-mediated regulation of SKN-1/Nrf in response to germ cell absence. eLife *4*.

956 Stroustrup, N., Ulmschneider, B.E., Nash, Z.M., Lopez-Moyado, I.F., Apfeld, J., and Fontana,
957 W. (2013). The Caenorhabditis elegans Lifespan Machine. Nat Methods *10*, 665-670.

958 Tatar, M., Bartke, A., and Antebi, A. (2003). The endocrine regulation of aging by insulin-like
959 signals. Science *299*, 1346-1351.

960 Tewari, M., Hu, P.J., Ahn, J.S., Ayivi-Guedehoussou, N., Vidalain, P.O., Li, S., Milstein, S.,
961 Armstrong, C.M., Boxem, M., Butler, M.D.*, et al.* (2004). Systematic interactome mapping and
962 genetic perturbation analysis of a C. elegans TGF-beta signaling network. Mol Cell *13*, 469-482.

963 Thomas, J.H., Birnby, D.A., and Vowels, J.J. (1993). Evidence for parallel processing of sensory
964 information controlling dauer formation in Caenorhabditis elegans. Genetics *134*, 1105-1117.

965 Trent, C. (1982). Genetic and behavioral studies of the egg-laying system in Caenorhabditis
966 elegans. Ph. D. Thesis, Massachusetts Institute of Technology.

967 Tullet, J.M., Hertweck, M., An, J.H., Baker, J., Hwang, J.Y., Liu, S., Oliveira, R.P., Baumeister,
968 R., and Blackwell, T.K. (2008). Direct inhibition of the longevity-promoting factor SKN-1 by
969 insulin-like signaling in C. elegans. Cell *132*, 1025-1038.

970 Tullio, F., Penna, C., Cabiale, K., Femmino, S., Galloni, M., and Pagliaro, P. (2017).
971 Cardioprotective effects of calcitonin gene-related peptide in isolated rat heart and in H9c2 cells
972 via redox signaling. Biomedicine & pharmacotherapy = Biomedecine & pharmacotherapie *90*,
973 194-202.

974 Uchida, O., Nakano, H., Koga, M., and Ohshima, Y. (2003). The C. elegans che-1 gene
975 encodes a zinc finger transcription factor required for specification of the ASE chemosensory
976 neurons. Development *130*, 1215-1224.

977 Veal, E.A., Day, A.M., and Morgan, B.A. (2007). Hydrogen peroxide sensing and signaling. Mol
978 Cell *26*, 1-14.

979 Wang, J., Robida-Stubbs, S., Tullet, J.M., Rual, J.F., Vidal, M., and Blackwell, T.K. (2010). RNAi
980 screening implicates a SKN-1-dependent transcriptional response in stress resistance and
981 longevity deriving from translation inhibition. PLoS genetics *6*.

982 West, S.A., Griffin, A.S., Gardner, A., and Diggle, S.P. (2006). Social evolution theory for
983 microorganisms. Nature reviews Microbiology *4*, 597-607.

984 White, J.G., Southgate, E., Thomson, J.N., and Brenner, S. (1986). The Structure of the
985 Nervous System of the Nematode C.elegans. Phil Trans Royal Soc Lond B *314*, 1-340.

986 Wolf, D.M., Vazirani, V.V., and Arkin, A.P. (2005). Diversity in times of adversity: probabilistic
987 strategies in microbial survival games. Journal of theoretical biology *234*, 227-253.

988 Wyatt, L.H., Luz, A.L., Cao, X., Maurer, L.L., Blawas, A.M., Aballay, A., Pan, W.K., and Meyer,
989 J.N. (2017). Effects of methyl and inorganic mercury exposure on genome homeostasis and
990 mitochondrial function in Caenorhabditis elegans. DNA repair *52*, 31-48.

991 Zinser, E.R. (2018). Cross-protection from hydrogen peroxide by helper microbes: the impacts
992 on the cyanobacterium Prochlorococcus and other beneficiaries in marine communities.
993 Environmental microbiology reports *10*, 399-411.

994 Zong, Y., Gao, J., Feng, H., Cheng, B., and Zhang, X. (2014). Toxicity of 7-ketocholesterol on
995 lethality, growth, reproduction, and germline apoptosis in the nematode Caenorhabditis elegans.
996 Journal of toxicology and environmental health Part A *77*, 716-723.

997

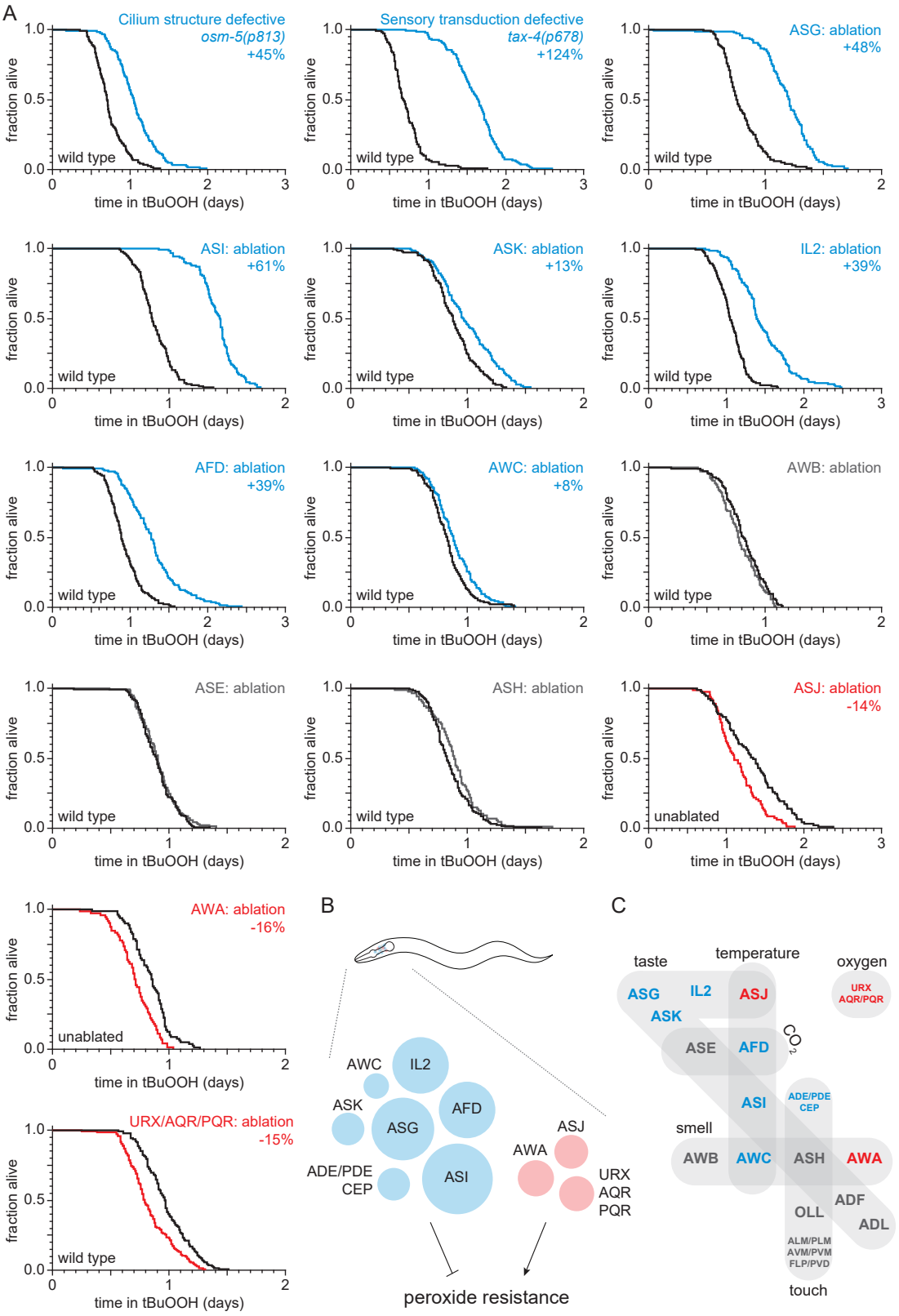

Figure 1. Sensory neurons regulate peroxide resistance in *C. elegans*

(A) Peroxide resistance of nematodes with defects in sensory cilia and sensory transduction, or with genetic ablation of specific sensory neurons. The fraction of nematodes remaining alive in the presence of 6 mM tert-butyl hydroperoxide (tBuOOH) is plotted against time. Interventions that

increased, decreased, or did not affect survival are denoted in blue, red, and gray, respectively, and their effects on mean peroxide resistance are noted.
(B) Specific sensory neurons normally reduce (blue) or increase (red) peroxide resistance. Circle area denotes the effect of ablation of the respective neuron on mean peroxide resistance.
(C) Sensory neurons are grouped by the stimuli they sense. Neurons that normally reduce (eight classes) or increase (three classes) peroxide resistance are shown in blue and red, respectively.
See also Figure S1. Statistical analyses are in Table S1.

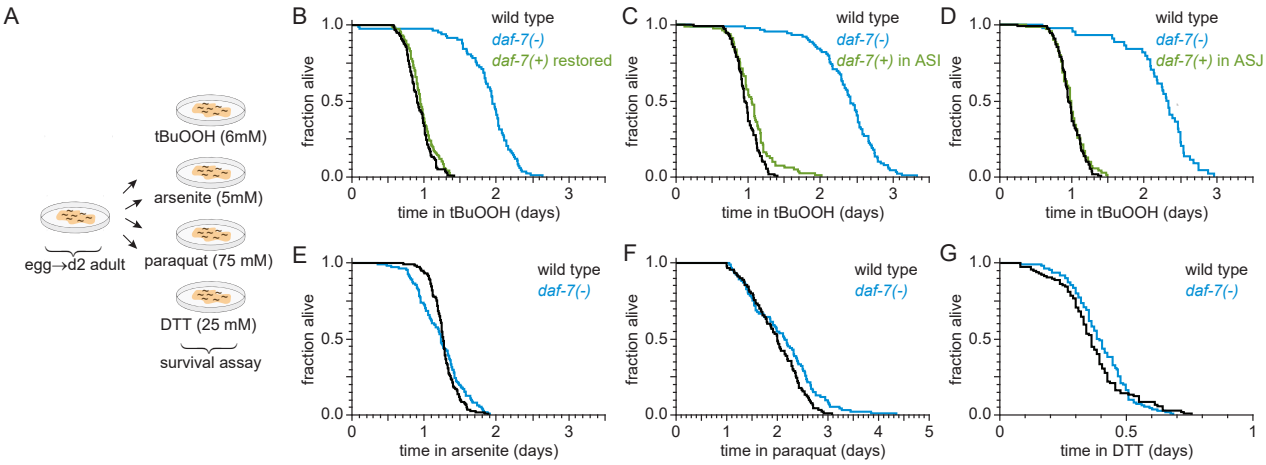

Figure 2. ASI sensory neurons secrete DAF-7/TGFβ to specifically lower the nematode's peroxide resistance

(A) Diagram summarizing experimental strategy.

(B-D) Peroxide resistance of wild type, *daf-7(ok3125)*, and *daf-7(ok3125)* with *daf-7(+)* reintroduced with (B) its endogenous promoter, (C) the ASI-specific *str-3* promoter, or (D) the ASJ-specific *trx-1* promoter.

(E-G) Resistance to 5 mM arsenite, 75 mM paraquat, and 25 mM dithiothreitol (DTT) of wild type and *daf-7(ok3125)*.

See also Figure S2. Statistical analyses are in Table S2.

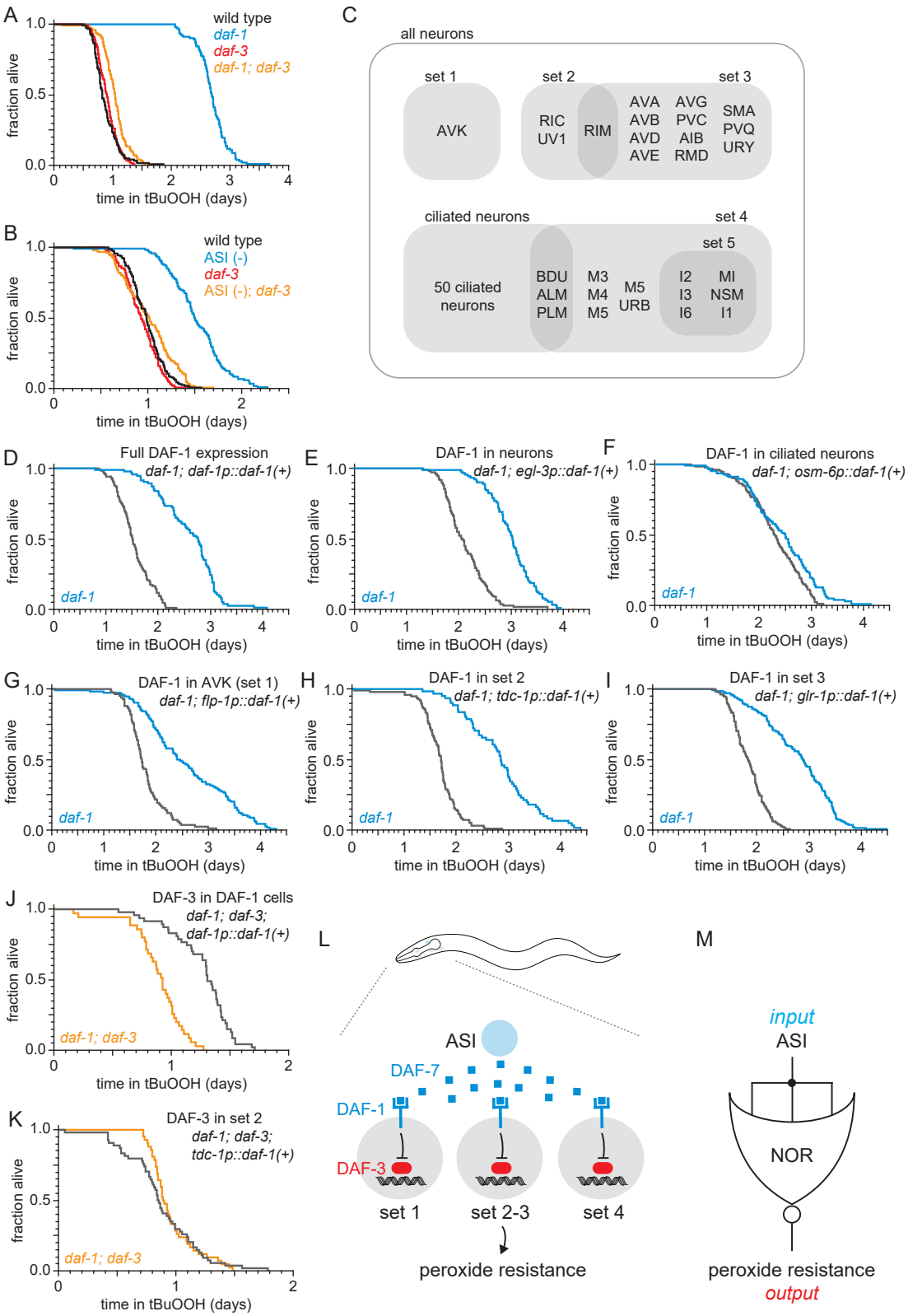

Figure 3. Interneurons must reach a consensus to increase peroxide resistance in response to DAF-7/TGFβ from ASI

(A-B) *daf-3(mgDf90)* almost completely abrogated the increased peroxide resistance of (A) *daf-1(m40)* and of (B) genetic ablation of ASI.

(C) Diagram of the subsets of neurons where *daf-1(+)* or *daf-3(+)* was expressed in transgenic rescue experiments shown in panels (D-K) and Figure S3. The *tdc-1* promoter also drives expression in the sheath cells of the somatic gonad.
(D-I) Peroxide resistance of transgenic nematodes expressing *daf-1(+)* in specific subsets of cells and *daf-1(m40)* controls.
(J-K) Peroxide resistance of transgenic nematodes expressing *daf-3(+)* in specific subsets of cells and *daf-1(m40); daf-3(mgDf90)* controls.
(L) ASI signals to three sets of interneurons to lower the nematode's peroxide resistance. To increase peroxide resistance, all of these sets of neurons must independently activate the DAF-3/DAF-5 transcriptional complex.
(M) ASI regulates the nematode's peroxide resistance via NOR logic gate implemented by sets of interneurons acting in parallel to receive and invert the DAF-7 signal from ASI.
See also Figure S3. Statistical analyses are in Table S3.

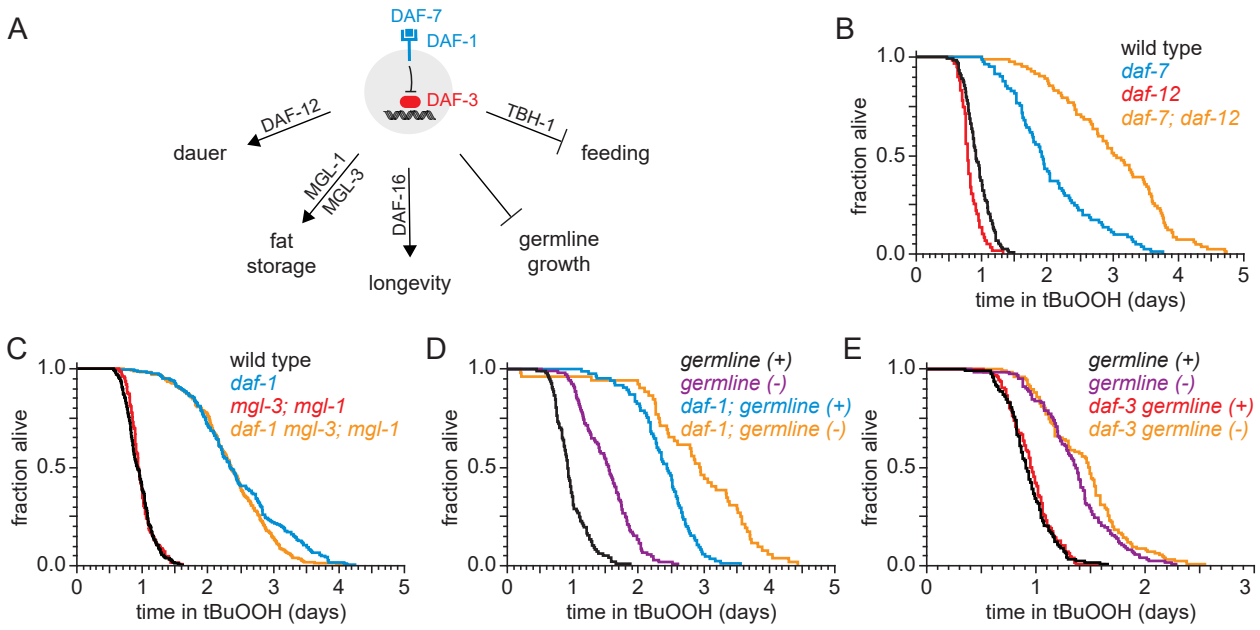

Figure 4. DAF-1/TGFβ-receptor signaling regulates peroxide resistance separately from its role in dauer formation, fat storage, and germline growth

(A) Different mechanisms operate downstream of DAF-3 to mediate the effects of DAF-7/TGFβ signaling on dauer-larva formation, fat storage, germline size, lifespan, and feeding.

(B) *daf-12(rh61rh411)* did not suppress the increased peroxide resistance of *daf-7(e1372)*.

(C) *mgl-1(tm1811)* and *mgl-3(tm1766)* did not jointly suppress the increased peroxide resistance of *daf-1(m40)*.

(D) Genetic ablation of the germline and *daf-1(m40)* independently increased peroxide resistance.

(E) *daf-3(mgDf90)* did not suppress the increased peroxide resistance of genetic ablation of the germline.

See also Figure S4. Statistical analyses are in Table S4.

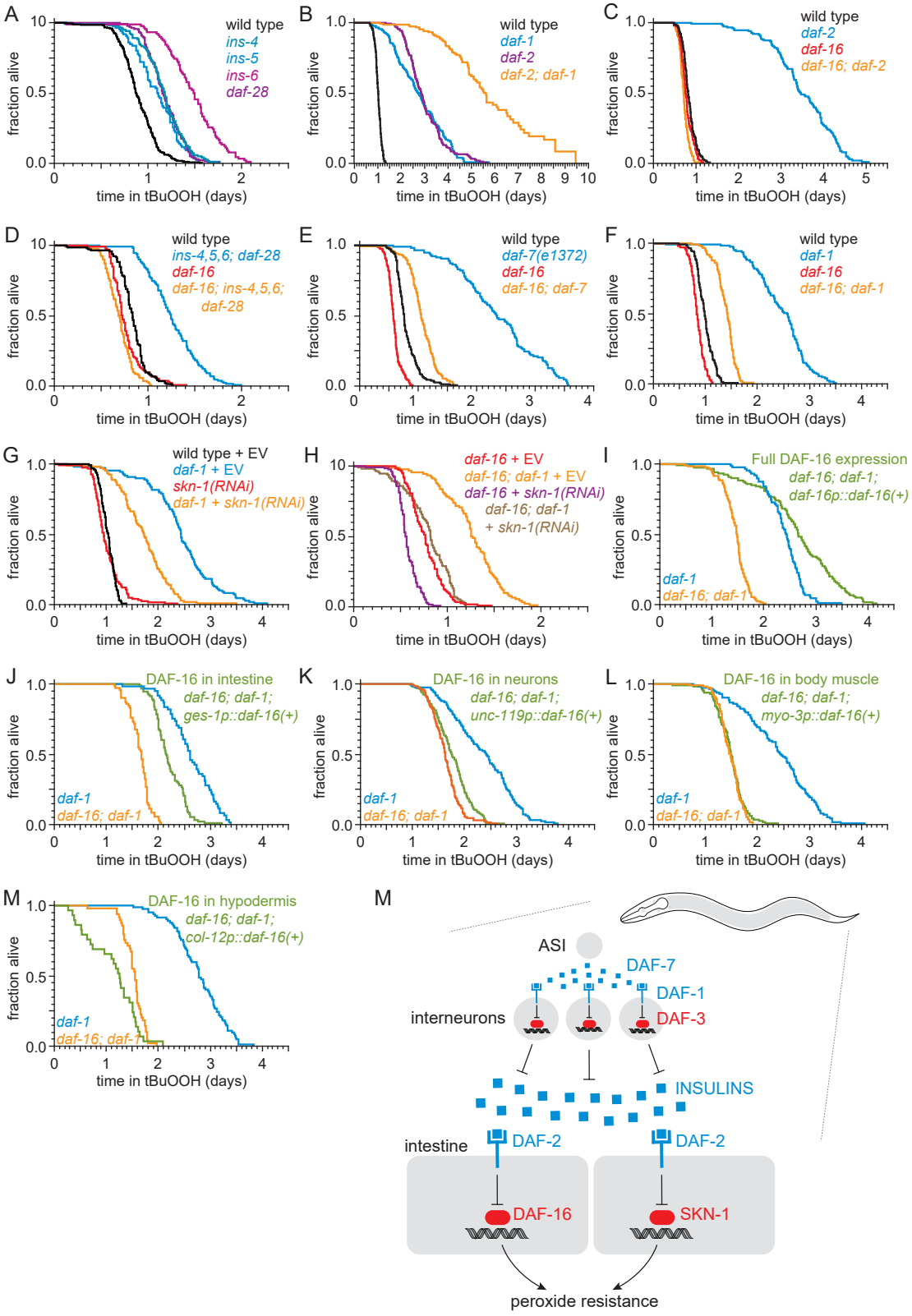

Figure 5. ASI regulates the nematode's peroxide resistance via a TGFβ-Insulin/IGF1 hormone relay

(A) Deletions in *ins-4, ins-5, ins-6,* and *daf-28* insulin-coding genes increased peroxide resistance.

(B) *daf-2(e1370)* and *daf-1(m40)* independently increased peroxide resistance.

(C-D) *daf-16(mu86)* abrogated the increased peroxide resistance of (C) *daf-2(e1370)* and (D) an *ins-4 ins-5 ins-6; daf-28* quadruple mutant.
(E-F) *daf-16(mu86)* suppressed part of the increased peroxide resistance of (E) *daf-7(e1372)* and (F) *daf-1(m40)*.
(G) *skn-1(RNAi)* suppressed part of the increased peroxide resistance of *daf-1(m40)*. Control RNAi consisted of feeding the nematodes the same bacteria but with the empty vector (EV) plasmid pL4440 instead of a plasmid targeting *skn-1*.
(H) *skn-1(RNAi)* lowered the peroxide resistance of *daf-16(mu86); daf-1(m40)*.
(I-M) Peroxide resistance of transgenic nematodes expressing *daf-16(+)* in specific subsets of cells, *daf-16(mu86); daf-1(m40)* controls, and *daf-1(m40)* reference.
(N) ASI sensory neurons make nematodes more sensitive to hydrogen peroxide via a multistep hormonal relay. DAF-7/TGFβ from ASI is received by interneurons. These interneurons act redundantly to relay this signal to target tissues by promoting transcription of insulin genes. These insulins activate the DAF-2 insulin/IGF1 receptor, leading to inhibition of DAF-16-dependent peroxide protection services by the intestine and neurons. SKN-1 acts independently of DAF-16 to promote peroxide resistance in response to reduced DAF-1 signaling. SKN-1 likely acts in the intestine, because *skn-1(+)* promotes peroxide resistance in *daf-2* mutants and induces oxidative-stress defenses in this tissue (An et al., 2005; Tullet et al., 2008).
See also Figure S5. Statistical analyses are in Table S5.

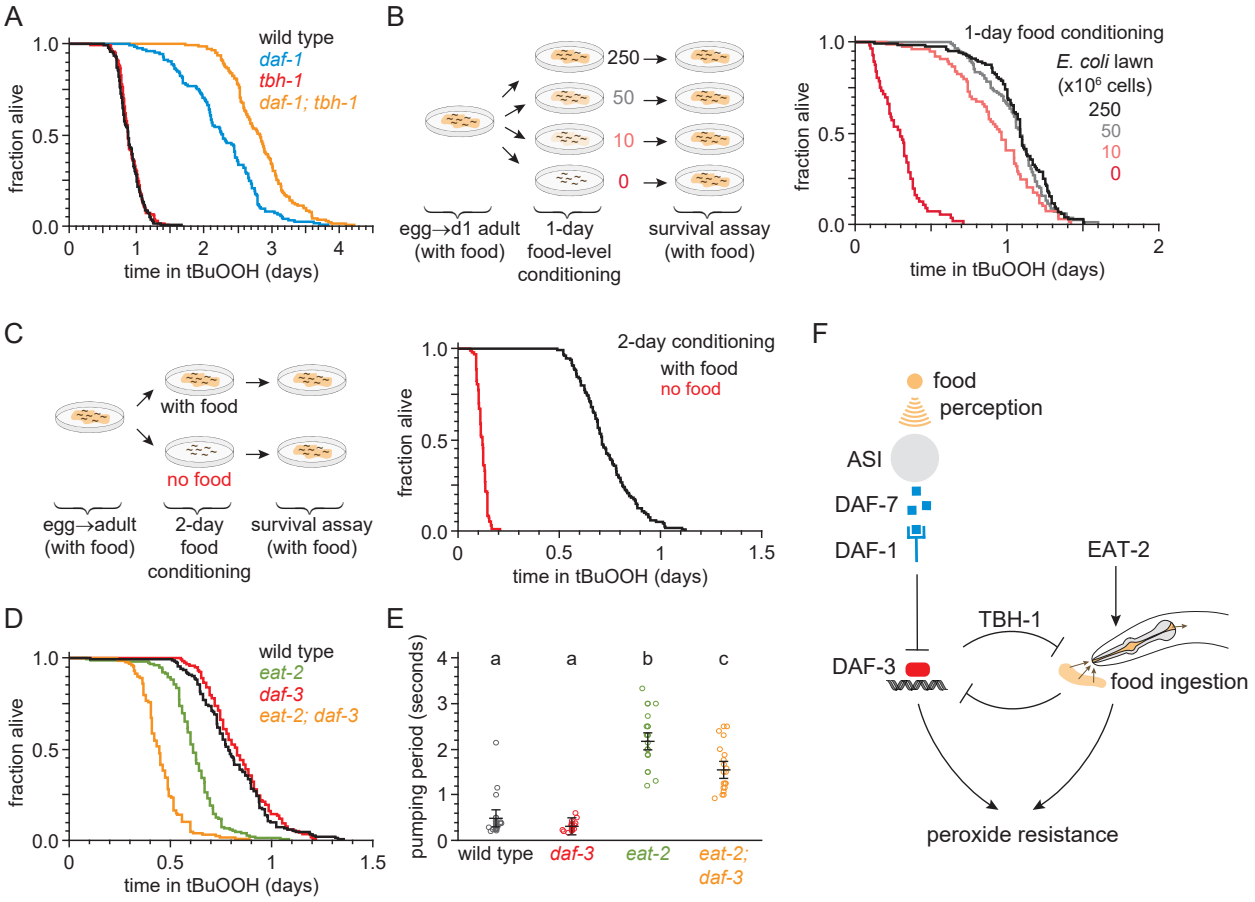

Figure 6. Food ingestion regulates the nematode's peroxide resistance via DAF-3/coSMAD
(A) *tbh-1(ok1196)* increased the peroxide resistance of *daf-1(m40)*.
(B-C) The *E. coli* level before the assay affected *C. elegans* peroxide resistance in a dose-dependent manner.
(D) *eat-2(ad1116)* caused a more severe reduction in peroxide resistance in *daf-3(mgDf90)* than in wild type.
(E) *eat-2(ad1116)* caused a less severe reduction in feeding in *daf-3(mgDf90)* than in wild type. Lines mark the mean pumping period and its 95% confidence interval. Genotypes labeled with different letters exhibited significant differences in pumping period ($P < 0.0001$, Turkey HSD test) otherwise ($P > 0.05$).
(F) DAF-3 and feeding increase peroxide resistance but attenuate each other's effects. Feeding inhibits DAF-3; this attenuates the reduction in peroxide resistance caused by reduced feeding. DAF-3 inhibits feeding via TBH-1; this attenuates the increase in peroxide resistance of *daf-1* mutants. Sensory perception of *E. coli* induces DAF-7 expression in (Chang et al., 2006; Gallagher et al., 2013) in a concentration-dependent manner (Entchev et al., 2015; Ren et al., 1996) leading to DAF-3 repression by the DAF-7 receptor DAF-1. Therefore, both ingestion and perception of *E. coli* inhibit DAF-3.
See also Figure S6. Additional statistical analyses are in Table S6.

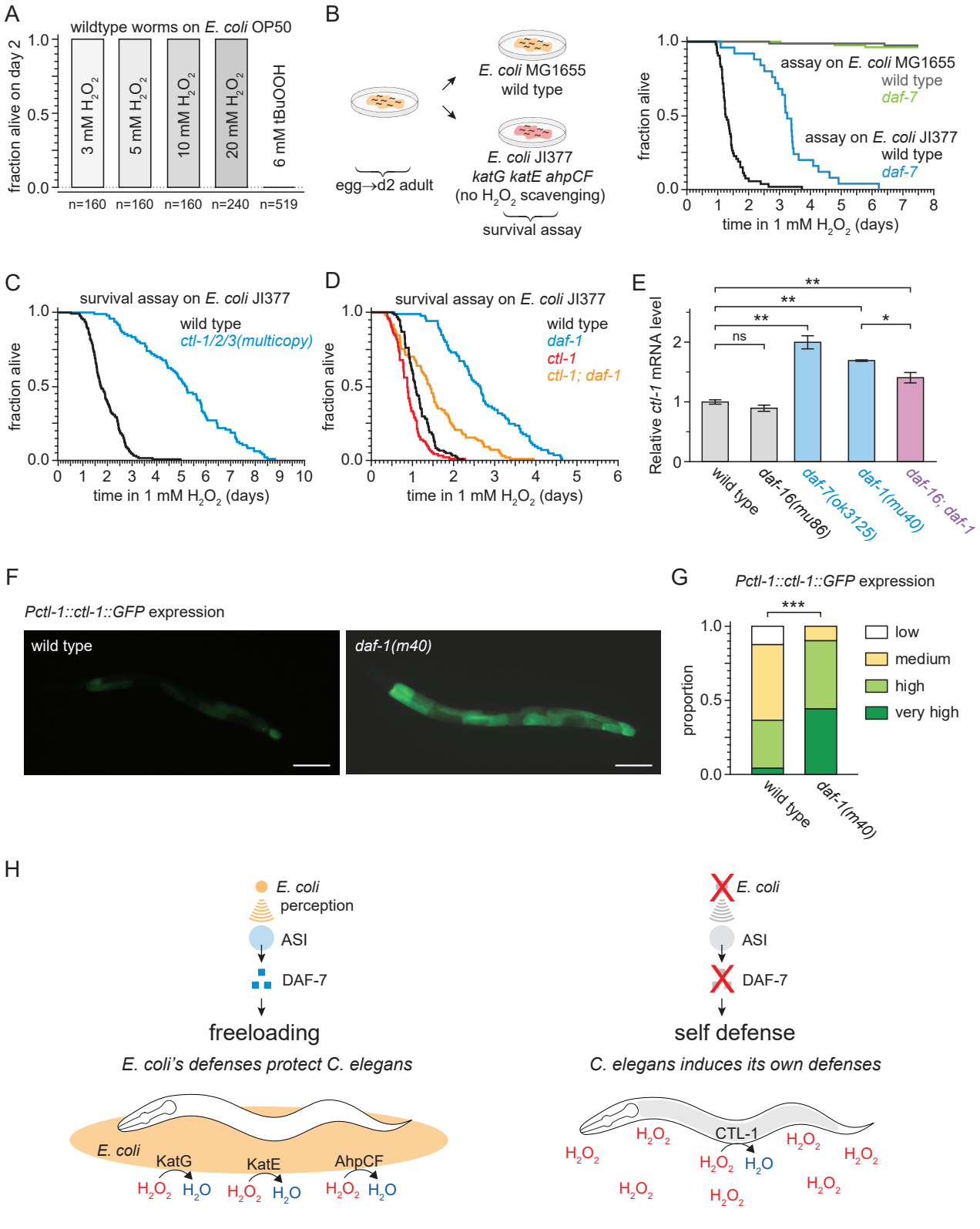

Figure 7. DAF-7/TGFβ signals that hydrogen-peroxide protection will be provided by catalases from *E. coli* and not by catalases from *C. elegans*

(A) *C. elegans* was sensitive to killing by tert-butyl hydroperoxide (tBuOOH), but not by hydrogen peroxide, in the presence of *E. coli* OP50.

(B) Hydrogen peroxide resistance of wild type and *daf-7(ok3125*) *C. elegans* in assays with wild type and *Kat*$^{-}$ *Ahp*$^{-}$ *E. coli*.
(C) Overexpression of the three endogenous catalases protects nematodes from hydrogen peroxide in assays with *Kat*$^{-}$ *Ahp*$^{-}$ *E. coli*.
(D) The cytosolic catalase *ctl-1(ok1242)* mutation suppressed part of the increased hydrogen peroxide resistance of *daf-1(m40)* in assays with *Kat*$^{-}$ *Ahp*$^{-}$ *E. coli*.
(E) DAF-7/TGFβ-pathway regulates *ctl-1* mRNA expression via DAF-16/FOXO, determined by quantitative RT-PCR. Data are represented as mean ± s.e.m of three independent biological replicates, each with three technical replicates. For comparisons of *ctl-1* mRNA expression between pairs of genotypes, ** indicates $P < 0.001$, * indicates $P < 0.05$, and "ns" indicates $P > 0.05$ (Turkey HSD test).
(F) Representative pictures of the expression of the *chIs166[Pctl-1::ctl-1::gfp]* reporter in wild type animals (left picture; category: medium) or *daf-1(m40)* mutants (right picture; category: very high). Scale bar = 100 µm.
(G) The expression of the promoter of *ctl-1* fused with GFP (*chIs166[Pctl-1::ctl-1::gfp]*) is higher in *daf-1(m40)* mutants (237 animals) than in wild type animals (145 animals), *** indicates $P < 0.0001$ (ordinal logistic regression). Scoring is described in Material and methods. See Figure S7C for representative pictures of each expression category.
(H) DAF-7/TGFβ signaling enables *C. elegans* to decide whether to induce its own hydrogen-peroxide defenses or, instead, freeload on protection provided by molecularly orthologous hydrogen-peroxide defenses from *E. coli*
See also Figure S7. Additional statistical analyses are in Table S7.